Not Just for Pulling Chromosomes:
The Role of Kinetochore-Microtubules in Enforcing Bipolarity of the Human Mitotic Spindle

By

Anna Sophia Gayek

Dissertation
Submitted to the Faculty of the
Graduate School of Vanderbilt University
in partial fulfillment of the requirements
for the degree of

DOCTOR OF PHILOSOPHY
in

Cell and Developmental Biology
May, 2016
Nashville, Tennessee

Approved:

Ryoma Ohi, Ph.D.

Irina Kaverina, Ph.D.

Chin Chiang, Ph.D.

Kathleen L. Gould, Ph.D.

Matthew J. Lang, Ph.D.

To my parents, Jon Gayek and Beth Hood, with love and gratitude

ACKNOWLEDGEMENTS

First and foremost, a huge “thank you” to my Ph.D. mentor, Ryoma “Puck” Ohi. I feel tremendously lucky to have learned lab techniques and scientific ways of thinking side-by-side with him at the bench in the early years of my graduate work. Without his creativity, enthusiasm, patience, and encouragement, this dissertation would not exist. Thanks also to Yaqing Du, Stephen Norris, Emma Sturgill, Jen Landino, and Megan Dumas, who set the example for collegial labmates and excellent scientists. My heartfelt appreciation goes out to the members of my committee, members of the Microtubules and Motors Club, and members of the Gould, M. Ohi, and Zanic laboratories for helpful discussions and suggestions. Special thanks go to the Vanderbilt Toastmasters Club for helping me become a more confident speaker.

Work in the Ohi lab is made possible by funding from the National Institute of General Medical Sciences. My PhD work was also supported by the Vanderbilt Graduate School and the Vanderbilt Molecular Biophysics Training Program (MBTP) – I thank Walter Chazin, director of the MBTP, both for financial support and for welcoming me into this community of scholars.

Finally, I’d like to extend my personal thanks to the people who kept me sane the past few years. In particular, Hannah Hankins, Amy Russo, Chauca English, Gwynne Davis and Peter Griffin celebrated with me when experiments worked, commiserated with me when experiments failed, and continually reminded me that there’s more to life than the lab. John Brooks taught me to seek out adventure and makes me excited for the years to come. My brother David, my oldest, best friend, always understood where I

was coming from. My parents not only gave me a wonderful early education and grounding in the world, but continued to provide moral support and encouragement in the face of grad school's frustrations. Many thanks to you all!

TABLE OF CONTENTS

LIST OF TABLES

LIST OF FIGURES

LIST OF ABBREVIATIONS

AO	Anaphase onset
A.U.	Arbitrary units
CAK	CDK-activating kinase
CDK	Cyclin-dependent kinase
CIN	Chromosomal instability
CLASP	Cytoplasmic linker associated protein
DMEM	Dulbecco’s Modified Eagle Medium
DMSO	Dimethyl sulfoxide
DPBS	Dulbecco’s phosphate-buffered saline
DNA	Deoxyribonucleic acid
FBS	Fetal bovine serum
FDAPA	Fluorescence dissipation after photoactivation
G0	Gap 0 (quiescence)
G1	Gap 1
G2	Gap 2
GST	Glutathione-S-transferase
HSET	Human spleen, embryo, and testes protein
hTERT	Human telomerase reverse transcriptase
HURP	Hepatoma upregulated protein
Kif	Kinesin family member
KLP	Kinesin-like protein

K-MT	Kinetochore-microtubule
M	Mitosis
MAP	Microtubule-associated protein
MCAK	Mitotic centromere-associated kinesin
MG-STLC	MG-132 followed by STLC
MT	Microtubule
NA	Numerical aperture
NEBD	Nuclear envelope breakdown
NuMA	Nuclear-mitotic apparatus protein
PBS	Phosphate-buffered saline
PBST	Phosphate-buffered saline with Tween
PCR	Polymerase chain reaction
PRC1	Protein regulator of cytokinesis-1
RNA	Ribonucleic acid
RNAi	RNA-interference
RPE-1	Retinal pigment epithelial cells
RPMI	Roswell Park Memorial Institute media
S	Synthesis
SAC	Spindle assembly checkpoint
SDS-PAGE	Sodium dodecyl sulfate polyacrylamide gel electrophoresis
s.e.m.	Standard error of the mean
siRNA	Small interfering RNA
STLC	S-trityl-L-cystein

TBST	Tris-buffered saline with Triton-X-100
TPX2	Targeting protein for XKLP2
XMAP215	*Xenopus* microtubule-associated protein of 215 kDa

CHAPTER 1

INTRODUCTION

Mitosis and the Cell Cycle

The human body is made up of over 3 x 10^{13} cells (Savage, 1977; Milo *et al.*, 2010). In addition, new cells are constantly being born to replace those that are damaged or shed: certain blood cells and cells of the intestinal epithelium, for example, turn over every 1-5 days (Flindt, 2006; Li *et al.*, 2011). These numbers reflect the tremendous proliferative potential of somatic cells, but also underscore the importance of proliferating accurately.

Eukaryotic cells proliferate through the ordered events of the cell cycle (Figure 1.1). In most cells, this cycle consists of a phase of growth and metabolic activity, called gap 1 (G1), followed by a DNA synthesis phase, called S phase, followed by a second gap phase, called G2. The DNA and cell contents are then split into two cells in mitosis, also called M phase. In HeLa human tissue culture cells, most of the cell cycle is spent in G1 (6-7 h) and S phase (8-9 h), with G2 lasting around 3 h, and mitosis being accomplished in less than 1 h (Hahn *et al.*, 2009). Cells can also exist in a quiescent or G0 phase, either to wait between rounds of division or to differentiate and carry out their functions (Oki *et al.*, 2014). On the opposite end of the spectrum, cells of the early embryo proliferate with almost no gap phases, proceeding directly from DNA synthesis to mitosis to DNA synthesis (Stead *et al.*, 2002).

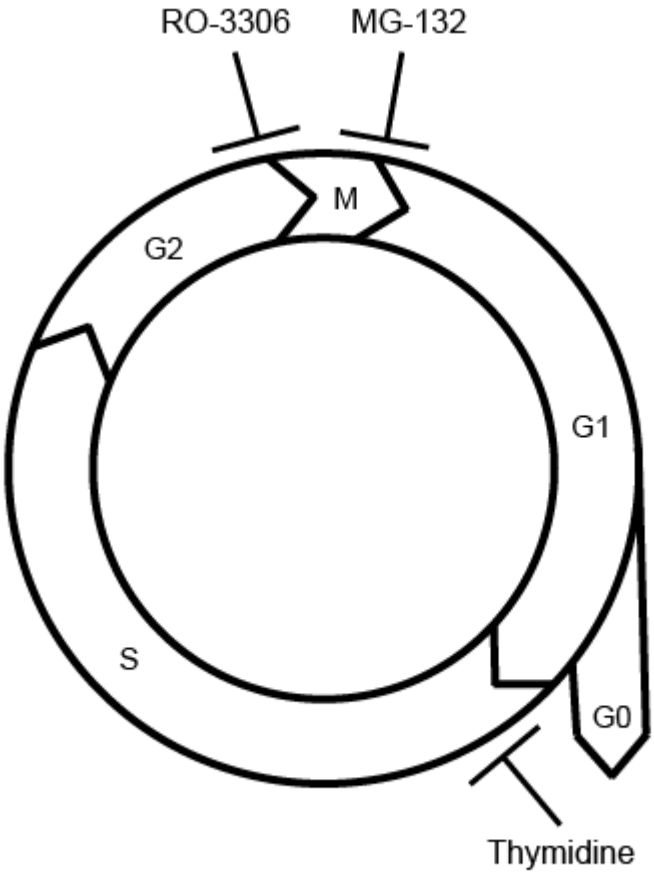

Figure 1.1: The cell cycle. Perturbations used in this study are shown at the point they arrest cells.

Progression through the cell cycle is controlled by the production of cyclin proteins and their association with cyclin-dependent kinases (CDKs) (Malumbres and Barbacid, 2009). Slow synthesis and rapid proteolysis of cyclins ensures that the cycle progresses only in one direction (Reed, 2003). Several cyclins, pairing with specific CDKs, are expressed in different stages of the cell cycle: in mammals, cyclin D pairs with CDK-4 and CDK-6 in G1, cyclin E pairs with CDK-2 to drive cells into S phase, cyclin A pairs first with CDK-2 in G2 and then with CDK-1 in early mitosis, and cyclin B pairs with CDK1 for mitotic entry and the bulk of mitotic control (Malumbres and Barbacid, 2009). Despite this preferential pairing between cyclins and CDKs, experiments in mice indicate that in vertebrates, most CDKs are dispensable for

production of most cell lineages: only CDK-1 deletion leads to a complete failure of embryonic cell proliferation (Santamaria *et al.*, 2007; Malumbres and Barbacid, 2009). This is reminiscent of the cell cycle control of the budding yeast *Saccharomyces cerevisiae*, where a single CDK (Cdc28) pairs with several cyclins to control cell cycle progression (Bloom and Cross, 2007).

To provide tighter control over the cell cycle, several regulatory proteins including kinases and phosphatases impact the activity of cyclin-CDK complexes. One of the best-studied mechanisms of additional control is in the case of mitotic entry. Some regulatory proteins, like the CDK-activating kinase (CAK), act constitutively (Tassan *et al.*, 1994). However, rather than gradually increasing at the rate of cyclin B production, the activity of cyclin B-CDK-1 abruptly increases at mitotic entry (Gavet and Pines, 2010). This cannot be explained solely by constitutively active regulatory proteins: instead, it is achieved by a feedback system in which CDK-1 both activates a protein that activates it, and inhibits a protein that inhibits it. Before mitosis, cyclin B-CDK1 is kept inactive by an inhibitory phosphorylation conferred by the kinase Wee1; as cells enter mitosis, this inhibitory phosphorylation is removed by the phosphatase Cdc25. Once cells achieve a small level of active CDK-1, it phosphorylates Wee1 to inhibit it, and phosphorylates Cdc25 to activate it, leading to rapid loss of inhibitory phosphorylation from other CDK-1 molecules (Lindqvist *et al.*, 2009).

Several perturbations are widely used to synchronize tissue culture cells at a given stage of the cell cycle. “Serum starvation” in media with reduced fetal bovine serum (FBS; a source of extracellular growth factors) induces some cell types to enter G0 (Rosner *et al.*, 2013). Treatment with excess thymidine, aphidicolin, or other factors

that block DNA synthesis arrest cells in S phase (Rosner *et al.*, 2013). Treating cells with broad-spectrum CDK inhibitors can block cells at several stages of the cell cycle (Villerbu *et al.*, 2002), but treating them with a specific CDK-1 inhibitor arrests them at the G2/M transition (Vassilev, 2006). Finally, cells can be arrested in mitosis either by blocking mitotic exit with drugs that prevent formation of the mitotic apparatus (nocodazole, taxol, Kinesin-5 inhibitors) or with drugs that prevent degradation of cyclin B, such as the proteasome inhibitor MG-132 (Potapova *et al.*, 2006; Rosner *et al.*, 2013). The perturbations used to synchronize cells in this study are noted in Figure 1.1.

There is a range of consequences that stem from errors in the accurate transmission of the genome to daughter cells. Damage to DNA or errors in DNA replication can lead to localized mutations which promote cancer and drive aging (Hoeijmakers, 2009). Errors in mitosis, however, can lead to the gain or loss of whole chromosomes, a state known as aneuploidy. Aneuploidy is highly correlated with cancer (Holland and Cleveland, 2012), although we still lack proof that gain or loss of a single chromosome can drive tumorigenesis. However, constitutively high rates of gain or loss of chromosomes, known as chromosomal instability (CIN), may promote tumorigenesis and tumor survival by allowing rapid changes in the genome (Holland and Cleveland, 2012; Santaguida and Amon, 2015). Errors in mitosis can also lead to individual chromosomes being packaged into micronuclei, small compartments distinct from the main nucleus, which can lead to their catastrophic reorganization in the following S phase (Thompson and Compton, 2011; Crasta *et al.*, 2012). Because mitotic errors can lead to such large-scale changes in the genome, it is critical to

understand the underpinnings of mitosis in order to understand how the genome is accurately transmitted through the cell cycle.

The Machinery of Mitosis

Similar to the stereotyped progression through the cell cycle, cells undergo a well-choreographed series of events within the phase of mitosis. As cells enter mitosis they undergo prophase, in which the chromosomes condense, the nuclear envelope breaks down, and cells prepare to build the mitotic spindle that will physically move the chromosomes into daughter cells. Spindles continue to be built through prometaphase, and are completely built by metaphase. At anaphase, the connections between sister chromatids (the duplicated chromosomes) are broken and chromatids segregate to opposite ends of the cell, and in telophase the cells reassemble nuclear envelopes around the chromosome masses and transition to G1. A process called cytokinesis separates the cytoplasm of the two cells, usually concurrently with anaphase and telophase. While these stages were originally identified morphologically, we now appreciate each stage as a distinct biochemical state (Kabeche and Compton, 2013; Wieser and Pines, 2015).

Cells prepare their genomes for mitosis through the processes of chromosome condensation and kinetochore assembly. As cells enter mitosis, their chromosomes condense from loose euchromatin, accessible for transcription, into tightly packed units to prevent tangling or tearing of the DNA (Bell and Straight, 2015). In addition, two specialized, layered protein plaques called kinetochores are built on each chromosome, one on each chromatid (Cheeseman, 2014). The innermost elements of the

kinetochore bind directly to a region of DNA called the centromere throughout the cell cycle, while intermediate elements load in S phase, and outer layers of the kinetochore are assembled only as the cell enters mitosis (Gascoigne and Cheeseman, 2013). The kinetochore serves to physically link chromosomes to the mitotic spindle, the macromolecular machine that generates the force to segregate the chromosomes. In addition, the kinetochore is a hub for the spindle assembly checkpoint (SAC), a biochemical signaling network that delays mitotic exit until all chromosomes are attached to the spindle (Musacchio and Salmon, 2007).

The bulk of the mitotic spindle is made of microtubules (MTs) (Inoue and Sato, 1967). These dynamic polymers have an innate polarity stemming from the polarity of their tubulin subunits (Amos and Klug, 1974; Nogales *et al.*, 1998). Both in cells and *in vitro*, the MT "plus" ends switch between phases of growth and shrinkage, or their dynamics can briefly pause (Cassimeris *et al.*, 1988; Walker *et al.*, 1988; Belmont *et al.*, 1990). Although the MT "minus" ends grow and shrink *in vitro* (Walker *et al.*, 1988), their dynamics *in vivo* have long been ignored and are only beginning to be understood. MTs' growth and shrinkage is termed "dynamic instability" because each MT within the population can be growing or shrinking despite the population being in the same biochemical milieu (Mitchison and Kirschner, 1984), and this dynamic instability is essential for their mitotic functions described below.

Microtubules in the spindle do not function alone – rather, they work in concert with hundreds of microtubule-associated proteins (MAPs). Some MAPs are critical for the nucleation of MTs in the spindle, including the gamma tubulin ring complex and augmin (Petry *et al.*, 2013). Other MAPs regulate the dynamics of MTs in the spindle,

including XMAP215, CLASP, and HURP (Gard and Kirschner, 1987; Sillje *et al.*, 2006; Maia *et al.*, 2012). Others, including NuMA, TPX2, and PRC1, help to crosslink and organize the microtubules of the spindle (Merdes *et al.*, 1996; Wittmann *et al.*, 2000; Zhu *et al.*, 2006).

In addition to noncatalytic MAPs, molecular motors play critical roles in the mitotic spindle. In most eukaryotes, members of the plus end-directed Kinesin-5 or Kinesin-12 families are required to build the spindle (discussed in more detail below). Members of the Kinesin-14 family and cytoplasmic dynein, both minus end-directed motors, keep the poles focused and regulate spindle length (Heald *et al.*, 1996; Goshima *et al.*, 2005; Cai *et al.*, 2009; Raaijmakers *et al.*, 2013). Plus end-directed members of the Kinesin-7, Kinesin-4, and Kinesin-10 families help to move the chromosomes towards the spindle equator (Levesque and Compton, 2001; Kapoor *et al.*, 2006). Finally, members of the Kinesin-4, Kinesin-8, and Kinesin-13 families modulate MT dynamics to ensure accurate attachment of kinetochores to MTs (Desai *et al.*, 1999; Du *et al.*, 2010; Stumpff *et al.*, 2012; Walczak *et al.*, 2013).

The MTs of the spindle are organized in a characteristic, bipolar pattern across eukaryotes (Figure 1.2). In mitotic spindles from fungi, plants, and mammals, the MTs are arranged with their minus ends gathered into two poles and their plus ends emanating toward the spindle equator (Euteneuer and McIntosh, 1981; Euteneuer *et al.*, 1982; Ding *et al.*, 1993; Winey *et al.*, 1995). In yeast, the minus ends are anchored at the two spindle pole bodies (Ding *et al.*, 1993); in animals, the majority of minus ends are anchored at the functionally homologous centrosomes (Euteneuer and McIntosh, 1981), although a few minus ends exist near the centrosome but not tethered to it

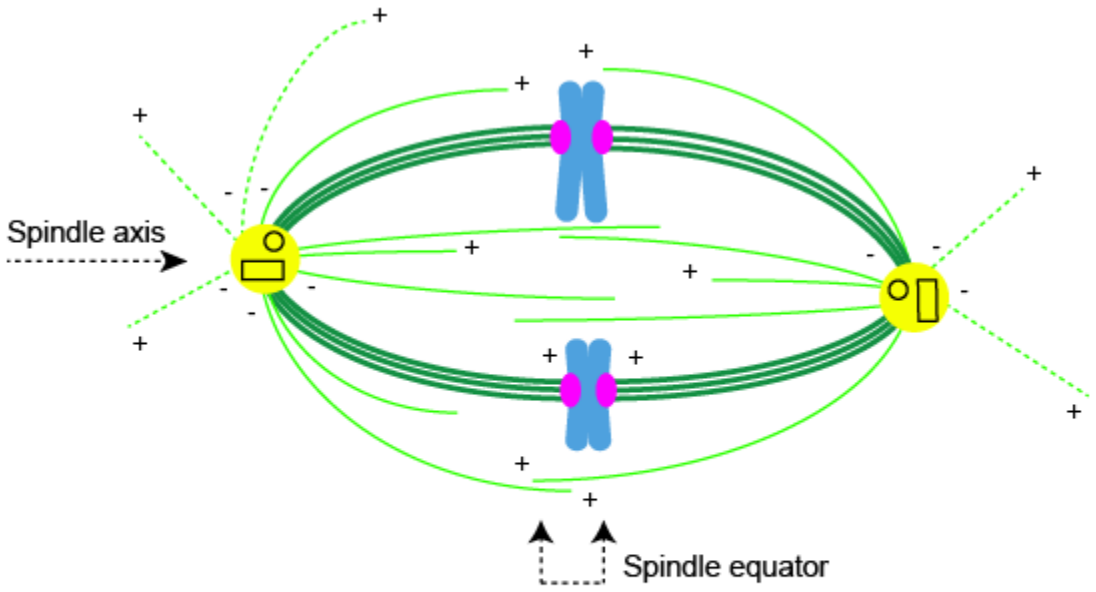

Figure 1.2. Schematic of the vertebrate mitotic spindle. K-MTs, non-K-MTs, and astral MTs are shown as dark green lines, pale green lines, and pale dashed green lines, respectively. Two duplicated chromosomes are shown in blue. Kinetochores are shown in magenta, and centrosomes are shown in yellow. Plus and minus ends of MTs are indicated. Not to scale.

(Mastronarde *et al.*, 1993; Sikirzhytski *et al.*, 2014). Although centrosomes are not required for vertebrate mitosis, when present they dominate minus end organization (Khodjakov *et al.*, 2000). In contrast to normal somatic mitotic spindles, vertebrate female meiotic spindles, studied most extensively in the *Xenopus laevis* egg extract system, form entirely without centrosomes (Gard, 1992). In addition, female meiotic spindles form as a tiled array of microtubules with their plus and minus ends distributed throughout the structure (Burbank *et al.*, 2006; Brugues *et al.*, 2012), instead of the strong polar or near-polar localization of minus ends in mitotic spindles. However, meiotic spindles share the overall bipolar geometry of mitotic spindles with minus ends denser near the pole they face (Brugues *et al.*, 2012). The bipolar geometry of the spindle allows us to define the spindle axis as the axis between the poles, and the spindle equator as the plane midway along the spindle axis and perpendicular to that axis.

Spindle microtubules are divided into three classes with different characteristics and functions (Figure 1.2). The most prominent class in mitotic cells is the kinetochore-microtubules (K-MTs), so called because their plus ends are embedded in the kinetochore structures described above (Dong *et al.*, 2007). In budding yeast, each kinetochore binds a single K-MT (Winey *et al.*, 1995), but in vertebrate animals each kinetochore binds a bundle of 20-30 MTs (McEwen *et al.*, 1997). The MTs in each K-MT bundle are parallel, meaning that their plus and minus ends are facing the same direction. The best-described functions of K-MTs are in moving the chromosomes and in silencing the SAC. The next class of spindle MTs is the non-kinetochore-microtubules (non-K-MTs, sometimes called interpolar MTs), MTs in the body of the spindle that do not attach end-on to kinetochores. In mitotic cells, non-K-MTs emanate from the poles toward or beyond the spindle equator, with MTs from each pole interdigitating in the middle of the spindle (Ding *et al.*, 1993; Mastronarde *et al.*, 1993). These interdigitating non-K-MTs are antiparallel; that is, the plus ends of MTs coming from one pole point in the same direction as the minus ends of MTs coming from the other pole. Non-K-MTs are a major substrate for mitotic motors and help the spindle establish its bipolar geometry (described below). The third major class of mitotic MTs is the astral microtubules, which emanate from the poles toward the cell cortex and are involved in positioning the spindle within the cell and positioning the cytokinetic furrow as cells exit mitosis (Grill *et al.*, 2001; Werner *et al.*, 2007).

While all classes of MTs are necessary for spindle function, K-MTs have a particularly important role in ensuring mitotic accuracy, because they are the major players in moving chromosomes. Kinetochores remain bound to K-MT ends as the MTs

depolymerize (Akiyoshi *et al.*, 2010), thereby coupling K-MT dynamics to movement of the chromosomes. K-MTs do not exert significant pushing forces on the chromosomes (Khodjakov and Rieder, 1996); rather, K-MT depolymerization pulls the chromosomes into alignment at the spindle equator and later to the poles in anaphase (Koshland *et al.*, 1988). Correct chromosome segregation requires the attachment of each of the two kinetochores on a chromosome to MTs coming from opposite poles. However, both kinetochores on a chromosome can attach to MTs coming from the same pole, meaning that both sister chromatids will go to the same daughter cell in anaphase (Musacchio and Salmon, 2007). Alternatively, because vertebrate kinetochores can bind 20-30 MTs, a single kinetochore can bind MTs coming from opposite poles, which will cause it to "lag" behind at the spindle equator while the rest of the chromosomes segregate to the poles in anaphase (Cimini *et al.*, 2001; Musacchio and Salmon, 2007). To avoid these errors, cells use biochemical cascades to disrupt incorrect K-MT attachments (Lampson *et al.*, 2004; Cimini *et al.*, 2006), and also build spindles in a way that predisposes kinetochores to form correct attachments (Magidson *et al.*, 2011).

In addition to growing and shrinking from their plus ends, MTs of the spindle also undergo a process called flux. Flux, the slow movement of polymerized tubulin from the center of the spindle to the poles, is conceptually similar to actin treadmilling (Mitchison, 1989): over time, subunits incorporated at one end of the fiber (in spindle MTs, the plus end) transition to being in the middle of the fiber, then at the opposite end (in spindle MTs, the minus end). However, unlike actin treadmilling, which is innate to the polymerization dynamics of the two ends, MT flux in the spindle requires the action of additional factors. In *Xenopus* egg extracts flux is driven by a Kinesin-5 motor

(Miyamoto *et al.*, 2004), but loss of this motor only mildly affects flux in mitotic mammalian tissue culture cells (Cameron *et al.*, 2006). Instead, molecules that promote plus end polymerization and minus end depolymerization have been proposed to drive flux in mitotic cells (Ganem and Compton, 2004; Wordeman *et al.*, 2007; Maffini *et al.*, 2009; Wang *et al.*, 2013). In *Drosophila* mitotic cells, flux plays a role in determining the size of spindles and in moving chromosomes to the poles in anaphase (Rogers *et al.*, 2004), but in vertebrate cells, flux has a subtler role in correcting incorrect K-MT attachments, and morphologically normal spindles can assemble without flux (Ganem *et al.*, 2005).

The different attachment states of K-MTs and non-K-MTs gives them quite different dynamic properties. Non-K-MTs undergo free dynamic instability as described above, with an average half-life of about 15 seconds (Kollu *et al.*, 2009; Kleyman *et al.*, 2014). K-MTs, on the other hand, persist with half-lives of 2-15 min (Bakhoum *et al.*, 2009a). The enhanced stability of K-MTs is partially attributable to kinetochore attachment itself, because tension applied through kinetochores promotes MT growth instead of shrinking (Akiyoshi *et al.*, 2010), and severed K-MTs rapidly depolymerize from their plus ends (Elting *et al.*, 2014; Sikirzhytski *et al.*, 2014). However, K-MT stability is also enhanced by several MAPs including Astrin and HURP (Sillje *et al.*, 2006; Thein *et al.*, 2007). K-MT stability can be keenly regulated by phosphorylation of kinetochore substrates and by MT-depolymerizing enzymes. A key player in this process is the Aurora B kinase, which phosphorylates MT-binding proteins at the kinetochore to promote their release from MTs (Lampson *et al.*, 2004; Cimini *et al.*, 2006; DeLuca *et al.*, 2011). In addition, the MT-depolmerizing Kinesin-13 members

MCAK and Kif2B can promote depolymerization of K-MT plus-ends leading to their release (Bakhoum *et al.*, 2009b).

Several techniques can be used to monitor the stability of MTs within the spindle. The enhanced stability of K-MTs is seen when cells are exposed to cold temperatures or Ca^{++}, which leads to the selective loss of non-K-MTs (Brinkley and Cartwright, 1975; Rieder, 1981; Gorbsky and Borisy, 1989; Lampson *et al.*, 2004). Differences in MT stability can also be more quantitatively measured using the technique of fluorescence dissipation after photoactivation (FDAPA), in which fluorescence of a photoactivatable tag on tubulin is locally activated in only a small region of the spindle. When corrected for photobleaching, loss of fluorescence from the activated region stems from the depolymerization of MTs in that region and diffusion of the fluorescent subunits out of the region (Zhai *et al.*, 1995; Bakhoum *et al.*, 2009a; Kabeche and Compton, 2013).

Within the broad range of their possible half-lives (2-15 min), K-MTs may turn over with very different kinetics depending on two system-level states. First, the stage of the cell cycle impacts K-MT turnover, with K-MTs turning over rapidly in prometaphase and becoming progressively more stable in metaphase and anaphase (Zhai *et al.*, 1995; Bakhoum *et al.*, 2009b; Kabeche and Compton, 2013). This progressive stabilization depends on degradation of the early-mitotic cyclin A (Kabeche and Compton, 2013), and may be effected by a change in K-MT regulating proteins at the kinetochore (Manning *et al.*, 2010). Second, the origin of the cells matters: “normal” or non-tumor-derived cells tend to have more unstable K-MTs than tumor-derived cells (Bakhoum *et al.*, 2009a). However, the molecular reason for K-MT hyperstability in

tumor-derived cells is not yet known, and there may be more than one possible route to the same hyperstable K-MT phenotype (Bakhoum *et al.*, 2009a).

K-MT stability must be tightly regulated to both satisfy the SAC and to allow accurate chromosome segregation. On the one hand, kinetochore attachment to MTs allows for satisfaction of the SAC and exit from mitosis (Tauchman *et al.*, 2015), so K-MT stability must be high enough that all kinetochores are attached at once. On the other hand, beyond the point necessary to satisfy the SAC, K-MT stability is inversely related to the accuracy of chromosome segregation: increasing K-MT stability increases the incidence of chromosomes that lag in anaphase (Bakhoum *et al.*, 2009b; Kabeche and Compton, 2013), which correlates with chromosome missegregation (Thompson and Compton, 2011). Cells must tightly regulate the stability of their K-MTs to balance SAC satisfaction with accurate K-MT attachment. Despite the importance of K-MT stability and our advances in understanding its regulation, we still are finding new mechanisms that regulate K-MT stability.

The Spindle Exists in a State of Force-Balance

As mentioned above, the spindle functions as a bipolar array of microtubules. Failure to form a bipolar spindle leads to disastrous consequences for the cell. Monopolar spindles, in which all the MT minus ends are gathered into a single focus, are incompetent for segregating chromosomes: vertebrate cells that form monopolar spindles either die by apoptosis or exit mitosis as tetraploid cells with double the normal number of chromosomes and centrosomes (Marcus *et al.*, 2005; Tao *et al.*, 2005; Gascoigne and Taylor, 2008). Tetraploid cells are more prone to missegregate chromosomes in subsequent mitoses (Ganem *et al.*, 2009), and a tetraploid

intermediate has long been envisaged as one route to tumorigenesis (Fujiwara *et al.*, 2005; Ganem *et al.*, 2007). On the other hand, cells that form multipolar spindles with more than two microtubule foci risk producing progeny with less than the full diploid genome content, which then die by apoptosis (Kwon *et al.*, 2008; Ganem *et al.*, 2009). Because bipolarity of the spindle is carefully balanced between the twin dangers of monopolarity and multipolarity, factors influencing spindle geometry have received considerable attention from researchers interested in both basic understanding and its translational potential.

Bipolarity of the spindle is established in most eukaryotes by members of the Kinesin-5 family. Kinesin-5 is organized as a dumbbell-shaped homotetramer with two motor heads on each end of a stalk, and it uses this geometry to slide antiparallel microtubules against each other to push the poles apart (Kapitein *et al.*, 2005). Mutation, depletion, or inactivation of Kinesin-5 from *Schizosaccharomyces pombe* (cut7), *Apergillus nidulans* (bimC), *Drosophila melanogaster* (KLP61F), *Xenopus* egg extracts (Eg5), or mammalian cells (Eg5) prevents the formation of bipolar spindles (Enos and Morris, 1990; Hagan and Yanagida, 1990; Sawin *et al.*, 1992; Heck *et al.*, 1993; Blangy *et al.*, 1995; Kapoor *et al.*, 2000). Because of this, intensive work has been focused on developing inhibitors to the human Kinesin-5, Eg5, as chemotherapies to block the proliferation of cancer cells. However, most Eg5 inhibitors so far have not been effective in clinical trials (Good *et al.*, 2015), perhaps because of compensation by another motor (described below). Despite their so-far lackluster performance in the clinic, Eg5 inhibitors have proven to be very useful in studying basic aspects of mitosis, including studies of not only spindle architecture but also kinetochore-microtubule

attachments, SAC inactivation, and cytokinesis (Kapoor *et al.*, 2000; Lampson *et al.*, 2004; Hu *et al.*, 2008; Tauchman *et al.*, 2015).

In only a few known cases, spindle assembly can proceed independently of Kinesin-5. In *Caenorhabditis elegans*, the single Kinesin-5 (BMK1) is not required for viability (Bishop *et al.*, 2005), and resists pole separation in anaphase rather than promoting pole separation in prometaphase (Saunders *et al.*, 2007). In place of Kinesin-5, a plus end-directed Kinesin-12 family member (KLP-8) is required to build bipolar spindles in *C. elegans* female meiosis (Segbert *et al.*, 2003), and dynein (presumably pulling on astral MTs) is required to build bipolar spindles in the early embryo (Gonczy *et al.*, 1999; Grill *et al.*, 2001; Yoder and Han, 2001). These same players, Kinesin-12 and dynein, can compensate for loss of Kinesin-5 function in human cells evolved to grow in the presence of Kinesin-5 inhibitors (Raaijmakers *et al.*, 2012; Sturgill and Ohi, 2013), but Kinesin-12 is required even in cells that also use dynein for initial pole separation. Overexpression of Kinesin-12 can also permit Kinesin-5-independent spindle assembly in human cells that have not been specially evolved to resist Kinesin-5 inhibitors (Tanenbaum *et al.*, 2009). Motivated by these findings that Kinesin-12 is the dominant factor for building bipolar spindles without Kinesin-5, members of our lab and others are actively searching for small molecules to inhibit the human Kinesin-12, called Kif15/Hklp2, in the hope of using combined Eg5 and Kif15 inhibition to block the proliferation of cancer cells resistant to Eg5 inhibitors alone (Groen, 2013; van Heesbeen and Medema, 2015).

The establishment of bipolarity is not enough for cells to accurately complete mitosis – the spindle must also maintain bipolarity until division is complete. In some

cases, inactivation of Kinesin-5 after cells have built a bipolar spindle leads to spindle collapse into monopolar structures. For instance, addition of Eg5-inactivating antibodies to *Xenopus* egg extracts leads to collapse of preformed bipolar spindles (Sawin *et al.*, 1992). Similarly, using heat to inactivate a temperature-sensitive Kinesin-5 mutant in fission yeast at metaphase causes the spindle to collapse (Syrovatkina *et al.*, 2013). This indicates that the bipolar spindle is not a static structure; rather, the force from Kinesin-5 pushing the poles outward is countered by other forces trying to pull the poles inward.

However, there are a few known cases where Kinesin-5 is required for establishment but not for maintenance of bipolarity. For instance, *Xenopus* egg extract spindles treated with the tubulin-sequestering protein Op18 form spindles devoid of non-K-MTs, and these are able to maintain bipolarity despite loss of Kinesin-5 activity (Houghtaling *et al.*, 2009). In addition, many common mammalian tissue culture cell models maintain bipolarity after inhibition of Eg5 (Kapoor *et al.*, 2000; Tanenbaum *et al.*, 2009; Vanneste *et al.*, 2009). In mammalian cells, maintenance of bipolarity without Eg5 requires Kif15 (Tanenbaum *et al.*, 2009; Vanneste *et al.*, 2009), in accordance with the necessity of Kinesin-12 for building bipolar spindles without Eg5.

The responses of cells to loss of Kinesin-5 activity have led to a model of the spindle in a balance of forces, with outward forces (pushing the poles apart) equaled by inward forces (pulling the poles together). Often these forces are thought of purely in terms of motor proteins (van Heesbeen *et al.*, 2014). Kinesin-5 is widely accepted as the major outward force generator, with Kinesin-12 acting as a secondary outward force generator. These are opposed by inward directed forces from dynein or Kinesin-14

(Mountain *et al.*, 1999; Sharp *et al.*, 2000; Tanenbaum *et al.*, 2008; van Heesbeen *et al.*, 2014).

However, a simple motor-centric view of force balance neglects the contribution of MTs themselves. MTs are known to produce force both from polymerization and from depolymerization (Dogterom and Yurke, 1997; Grishchuk *et al.*, 2005). For instance, MT polymerization helps to correctly position nuclei in yeast (Tran *et al.*, 2001). In addition, MT depolymerization is known to have a critical role in the spindle: depolymerization of K-MTs pulls the chromosomes into alignment at metaphase and to the poles in anaphase (Koshland *et al.*, 1988).

Changes in MT dynamics are known to impact the ability of cells to form or maintain bipolar spindles. Changes in MT dynamics also are known to impact the length of spindles, which may reflect milder changes in the same forces that shape the spindle's bipolar architecture. However, a clear picture of the role of MT dynamics has yet to emerge. For instance, in some cases destabilization of non-K-MTs promotes spindle bipolarity. Depletion of the MT-depolymerizing Kinesin-13 MCAK promotes bipolar spindle collapse in human cells when Eg5 is inhibited, an effect proposed to occur by increasing the overlap length of interdigitating non-K-MTs, allowing for more inwards pulling by dynein (Kollu *et al.*, 2009). However, in other cases extra non-K-MTs promote bipolarity in the absence of Eg5 function: perturbation of MT dynamics allows the formation of acentrosomal MT asters in human cells, which can act as an intermediate in Kif15-dependent, Eg-5-independent bipolarization (Florian and Mayer, 2011). Likewise, in *Drosophila* S2 cells, depletion of MT-stabilizing factors led to shorter

spindles, while depletion of MT-destabilizing factors made spindles longer (Goshima *et al.*, 2005).

Similarly, perturbations of K-MT stability have produced conflicting results on bipolarity. At the most basic level, blocking formation of kinetochore-to-MT attachments increases spindle length in human and yeast cells (DeLuca *et al.*, 2002; Syrovatkina *et al.*, 2013), and blocking release of kinetochore-to-MT attachments slows the process of bipolarization (Zaytsev *et al.*, 2014), suggesting that K-MTs pull the poles inward. This is in agreement with the role of K-MTs in pulling chromosomes: Newton's third law tells us that when K-MTs anchored at the pole pull on chromosomes, the chromosomes pull back in on the pole. Likewise, unbalanced flux of K-MTs, with depolymerization at one MT end not matched by polymerization at the other end, has been proposed to pull the poles inwards to create shorter or monopolar spindles (Waters *et al.*, 1996; Ganem and Compton, 2004). However, flux of K-MTs has also been suggested to push the poles apart, with the incorporation of tubulin subunits at K-MT plus ends thrusting the minus ends outward (Toso *et al.*, 2009). Although K-MT attachment and spindle bipolarity are both critical for successful mitosis, a unifying model for how K-MT stability regulates bipolarity remains to be established.

Why would cells evolve spindles in such a complicated force-balance if it makes them vulnerable to Kinesin-5 inhibition at metaphase? First, force-balance is important for avoiding multipolar spindles: overexpression of either Eg5 (Drosopoulos *et al.*, 2014) or Kif15 (personal observation) generates multipolar spindles in human cells. Force-balance is also important for forming correct K-MT attachments. Human cells in which Eg5, Kif15, and dynein have all been depleted or inactivated can form bipolar spindles

before Eg5 inactivation, but fail to then satisfy the SAC (van Heesbeen *et al.*, 2014), likely through a failure to form or maintain MT attachments to all kinetochores (Tauchman *et al.*, 2015). In fission yeast and human cells, perturbing molecular motors to slightly change spindle length impacted the frequency of incorrect K-MT attachments (Choi and McCollum, 2012). The interplay between force-balance, bipolarity, and K-MT attachment stability is critically important for successful mitosis, yet is not well understood.

In this study, we add to our understanding of the interplay between K-MT attachment stability and spindle force-balance by showing that in human cells, high K-MT stability promotes bipolar spindle maintenance despite loss of Eg5 activity, while low K-MT stability promotes bipolar spindle collapse. This underlies the differences in the ability of cell lines to maintain bipolarity without Eg5. We also show that inhibition of CDK-1 during the G2 phase of the cell cycle promotes K-MT stabilization and thereby promotes bipolar spindle maintenance. While there is much work still to be done to understand how K-MT stability impacts the maintenance of bipolarity without Eg5, this work shows that K-MT stability plays an important role in the balance of forces of the mitotic spindle

CHAPTER 2

MATERIALS AND METHODS

Cell Culture and Transfections

All cell lines were grown in media supplemented with 10% FBS and antibiotics. Media for RPE-1/mCherry-tubulin stable cells was additionally supplemented with 500 µg/mL G418. HeLa "Kyoto," c33A, HCT116, and BJ-hTERT cells (a gift from Dr. David Cortez, Vanderbilt University Medical Center) were cultured in DMEM. RPE-1 cells were cultured in 50% DMEM / 50% Ham's F-12 (Chapter 3) or in 100% DMEM (Chapter 4). U2OS cells were cultured in McCoy's 5A. CaSki cells were cultured in RPMI.

DNA transfections of HeLa and RPE-1 cells were performed using Lipofectamine 2000 (Invitrogen) or Fugene 6 (Roche), respectively, according to the manufacturer's instructions. siRNA transfections were performed with HiPerFect (Qiagen) according to the manufacturer's instructions. The siRNA sequences used are shown in Table 2.1. Before siRNA transfection, RPE-1 cells were serum-starved in DMEM supplemented with antibiotics but no serum for 6-8 h before transfection, at which time serum was returned. Cells were used 48 h (HeLa) or 72 h (RPE-1) after siRNA transfection.

A polyclonal RPE-1 cell line expressing mCherry-tubulin was generated by first selecting stably transfected cells with G418, followed by flow cytometry to select for fluorescence positive cells. Flow cytometry was performed in the Vanderbilt University Medical Center Flow Cytometry Shared Resource.

Target	Sequence	Source	Reference
Astrin	TCCCGACAACTCACAGAGAAA	Qiagen	(Thein *et al.*, 2007)
Kif15	GGACAUAAAUUGCAAUACUU	Dhamacon	(Tanenbaum *et al.*, 2009)
HURP	CCAGUUACACCUGGACUCCUUUAAA	Invitrogen	(Ye *et al.*, 2011)
Nuf2	AAACGAUAGUGCUGCAAGA; GGAUUGCAAUAAAGUUCAA; UAGCUGAGAUUGUGAUUCA; GAACGAGUAACCACAAUUA (ON-TARGET plus SMARTpool)	Thermo Scientific	
LoGC Duplex Scrambled	proprietary	Invitrogen	
LoGC Duplex #2 Scrambled	proprietary	Invitrogen	
AllStars Negative Control	proprietary	Qiagen	

Table 2.1. Sequences of siRNAs used in this study.

Drugs

Drug stocks were stored at -20°C and diluted in media promptly before use. Drug concentrations, sources, and treatment times are shown in Table 2.2. Cytochalasin B was washed out with 6 washes over the course of 30 min; this was adapted from a published method (Yi et al., 2011). Thymidine was washed out with 2 washes and RO-3306 was washed out with 5 washes. All drug treatments were performed at 37°C under culturing conditions.

Generation of centrin antibodies

Centrin 1 (GenBank Accession Number BC084063) was PCR amplified from a *Xenopus laevis* ovary cDNA library (a gift from A. Straight, Stanford University) and expressed in BL-21(DE3) cells as a GST fusion protein. GST-Centrin was purified on glutathione agarose (Sigma) and used to immunize rabbits (Cocalico). Centrin-specific

antibodies were affinity purified by passing anti-GST-depleted serum over Affi-Gel 10 (Bio-Rad) covalently coupled to GST-Centrin. Affinity-purified antibodies were dialyzed into PBS, frozen in liquid nitrogen, and stored at -80°C. We thank Chauca English for assistance in preparing these antibodies.

Drug	Source	Solvent	Working concentration	Duration
MG-132	CalBioChem	DMSO	5 μM	90 min - 5 h
STLC	Sigma-Aldrich	DMSO	10 μM (Chapter 3), 80 μM (Chapter 4)	2-90 min
Taxol	Sigma-Aldrich	DMSO	2.5 nM (Chapter 3), 0.5 nM (Chapter 4)	90 min - 5 h
Nocodazole	Sigma-Aldrich	DMSO	5 μM	6 min
Cytochalasin B	Sigma-Aldrich	DMSO	3 μg/mL	24 h
Thymidine	Sigma-Aldrich	Water	2 mM	16-24 h
RO-3306	Axxora	DMSO	9 μM	1-12 h

Table 2.2. Drugs used in this study.

Antibodies

Additional primary antibodies are shown in Table 2.3. Species-appropriate secondary antibodies conjugated to Alexa 488, Alexa 594, Alexa 647 (for immunofluorescence), or to Alexa 700, Alexa 750, or Alexa 800 (for immunoblotting) were purchased from Invitrogen.

Immunoblotting

Lysates were prepared by washing cells three times with DPBS, suspending them in 2X Laemmli buffer, and boiling them for 5 min. Mitotic lysates were prepared by

Antibody	Source	Dilution
Mouse anti-tubulin, DM1alpha monoclonal	Vanderbilt Antibody and Protein Resource	1:500
Mouse anti-gamma-tubulin, GTU88 monoclonal		1:1000
Mouse anti-Hec1, 9G3 monoclonal	AbCam	1:1000
Rat anti-tubulin, YL1/2 monoclonal	Accurate Chemical and Scientific Corporation	1:1000
Rabbit anti-centrin	This study	1:1500
Rabbit anti-Kif15	(Sturgill and Ohi, 2013)	1:2000
Rabbit anti-Eg5	(Miyamoto *et al.*, 2004)	1:1000
Rabbit anti-astrin	Santa Cruz Biotechnologies	1:100
Rabbit anti-HURP (Western blots)	Bethyl Labs	1:1000
Goat anti-HURP (immuofluorescence)	Santa Cruz Biotechnologies	1:100
Human autoimmune serum, CREST	ImmunoVision	1:1000

Table 2.3. Primary antibodies used in this study.

synchronizing cells with a thymidine block; ten hours after thymidine washout, cells were arrested in mitosis for 3 h in 10 μM STLC; plates were rinsed three times in DPBS; and mitotic cells were collected by shake-off, lysed in 2X Laemmli buffer, and boiled as above. Proteins were resolved by SDS-PAGE and transferred to nitrocellulose membranes. Membranes were blocked with Odyssey Blocking Buffer (Licor Biosciences), probed with primary antibodies diluted in 5% w/v milk in PBST for 1 h, then probed with species-appropriate fluorescently tagged secondary antibodies in PBST+milk for 45 min. Fluorescence was measured with an Odyssey fluorescence detection system (Mandel Scientific).

Immunofluorescence and Fixed Cell Imaging

Cells subjected to nocodazole shock were permeabilized for 20 s at room temperature in 100 mM K-PIPES, pH 6.8, 0.4% Triton-X 100, 10mM K-EGTA, 1mM $MgCl_2$ immediately before fixation. All cells were fixed in methanol at -20°C for 10 min. Rinses were performed with TBS+0.1% Triton-X 100 (TBST). Coverslips were blocked with AbDil (TBST + 2 mg/mL bovine serum albumin (Sigma-Aldrich)) for 10 min, probed with primary antibodies diluted in AbDil for 1 h, rinsed, probed with secondary antibodies diluted in AbDil for 45 min, and rinsed. DNA was stained with 5 µg/mL Hoechst 33342. Coverslips were mounted in Prolong Gold (Invitrogen).

Fixed cells were imaged using a 60X 1.4 NA objective (Olympus) with 1.6X auxiliary magnification on a DeltaVision Elite imaging system (Applied Precision). Optical sections were collected every 0.2 nm. Ratio deconvolution and maximum-Z projection were performed in SoftWorx (Applied Precision). Images were prepared for publication using ImageJ and NIS-Elements (Nikon) software. All images are maximum-Z projections of deconvolved image stacks. Quantification of spindle intensity was performed in NIS-Elements: for a single, central Z-plane, the average fluorophore intensity of the non-spindle cytoplasm was subtracted from the average fluorophore intensity of the spindle.

Live Cell Imaging

For imaging of spindle maintenance or collapse, cells were plated to MatTek dishes (MatTek Corporation). HeLa cells were transfected with mCherry-tubulin ~24 h after plating and imaged 48 h after plating. RPE-1/mCherry-tubulin stable cells were

imaged 24-48 h after plating. Cells were imaged at 37°C with ~5% CO_2 using a 60X 1.4 NA objective (Olympus) on a DeltaVision Elite imaging system equipped with a WeatherStation environmental chamber (Applied Precision). 100 min before imaging, culturing media was exchanged for 5 μM MG-132 in 1 mL movie medium (L-15 media without phenol red supplemented with 10% FBS, antibiotics, and 7 mM K-HEPES, pH 7.7). Immediately before imaging, an additional 1 mL movie medium with 5 μM MG-132 and 20 μM STLC was added. Several fields of view were chosen; for each field of view 5 optical sections, 1.5 μM apart, were imaged every 90 sec for 1 h. Maximum-Z projections are shown.

For imaging of mitotic timing, cells were imaged at 37°C with ~5% CO_2 using a 40X 1.3 NA objective (Olympus) on a DeltaVision Core imaging system equipped with a WeatherStation environmental chamber (Applied Precision). For Chapter 3, RPE-1 cells were plated to MatTek dishes and imaged 24 h after plating. One hour before imaging, culture medium was exchanged for 2 mL movie medium with or without 2.5 nM taxol. Immediately before imaging, the dish lid was removed and the medium was overlaid with mineral oil. Several fields of view were chosen; for each field of view, 4 optical sections, 2 μm apart, were imaged every 3 min for 5 h. For Chapter 4, cells were plated to MatTek dishes, subjected to a double thymidine block, released for 5 h into complete DMEM, treated for 3 h with 9 μM RO-3306 or DMSO in DMEM, and washed; DMEM was exchanged for 2 mL movie media, the dish lid was removed, the media was overlaid with mineral oil, and several fields of view were imaged as 2 optical sections, 2 μm apart, every 3 min for 3 h.

Statistical Analysis

T-tests (two-tailed, assuming unequal variance) were performed with the TTEST function in Excel (Microsoft).

CHAPTER 3

KINETOCHORE-MICROTUBULE STABILITY GOVERNS THE METAPHASE REQUIREMENT FOR EG5

A. Sophia Gayek and Ryoma Ohi

Department of Cell and Developmental Biology, Vanderbilt University Medical Center, Nashville, TN 37232

Previously published as:

Gayek A.,S., Ohi R. (2014) Kinetochore-microtubule stability governs the metaphase requirement for Eg5. *Mol Biol Cell* 25, 2051-60.

Eg5 is essential for robust maintenance of spindle bipolarity in some cell types

Eg5 has been reported to be dispensable for maintaining spindle bipolarity in human cells, but this has only been tested in a few cell lines (Blangy *et al.*, 1995; Kapoor *et al.*, 2000; Kollu *et al.*, 2009; Tanenbaum *et al.*, 2009; Vanneste *et al.*, 2009). To determine if Eg5 is universally dispensable for maintaining spindle bipolarity in human cells, we used an assay (Tanenbaum *et al.*, 2009) that tests the ability of metaphase cells to maintain spindle bipolarity upon exposure to S-trityl-L-cysteine (STLC), a small molecule inhibitor of Eg5 (DeBonis *et al.*, 2004). Briefly, we treated a panel of human cell lines with the proteasome inhibitor MG-132 for 90 min to allow for bipolar spindle assembly, and then treated the cells with MG-132 and STLC for a further 90 min (Figure 3.1A; MG-STLC). An identical treatment using DMSO in place of STLC was used as a vehicle control (Figure 3.1A; MG-DMSO). A 90 min treatment with MG-132 causes accumulation of mitotic cells at metaphase by blocking Cyclin B degradation, so STLC application chiefly impacts bipolar spindle maintenance rather than bipolar spindle formation.

We found that human cell lines have different capacities to maintain spindle bipolarity in the absence of Eg5 activity. In accordance with prior reports, most spindles were bipolar after MG-STLC treatment in HeLa (84.3±2.3%, mean±SEM; n=300), U2OS (94.0±1.5%; n=300), HCT116 (89.0±3.4%; n=300), and c33A cells (86.0±1.2%; n=400; Figure 3.1, B and D). Unexpectedly, most spindles were monopolar after the same drug treatments in RPE-1 (79.7±6.8%; n=300), BJ (97.3±2.2%; n=300), and CaSki cells (81.0±2.7%; n=400; Figure 3.1, C and D), suggesting that Eg5 is necessary for efficient bipolar spindle maintenance in these cell lines. Importantly, resistance to STLC cannot

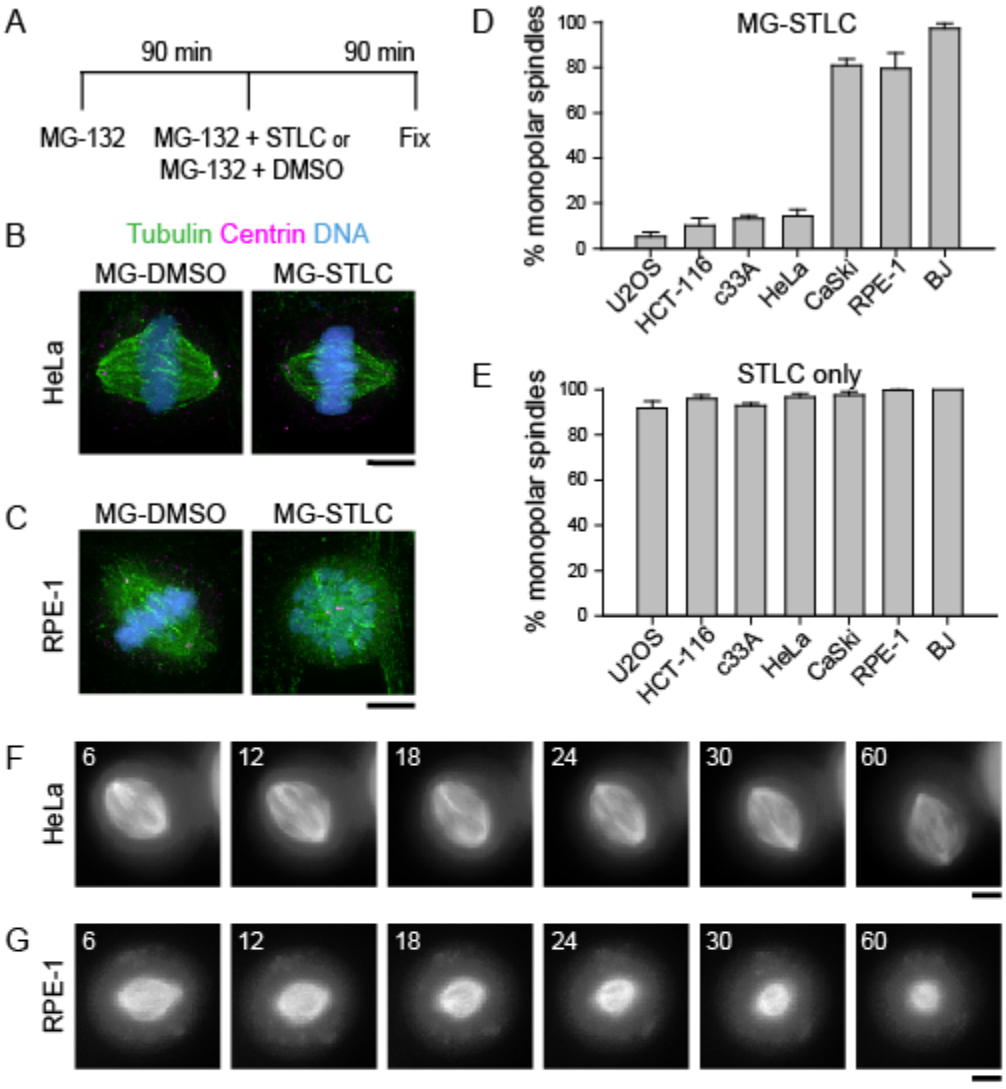

Figure 3.1. The ability of human cell lines to maintain spindle bipolarity in the absence of Eg5 activity varies. A) Bipolar spindle collapse assay. Cells were arrested in mitosis for 90 min with 5 μM MG-132, then treated for an additional 90 min with 5 μM MG-132 plus 10 μM STLC to inhibit Eg5 ("MG-STLC") or with 5 μM MG-132 plus DMSO equal in volume to STLC ("MG-DMSO"), and fixed. B and C) Representative images of HeLa (B) or RPE-1 (C) cells treated with MG-DMSO or MG-STLC. Tubulin (green) and centrin (magenta) were detected by immunostaining. DNA (blue) was counterstained with Hoechst 33342. Scale bar, 5 μm. D) Quantification of spindle geometries following MG-STLC treatment as described in (A). Data represent the mean ± SEM; n≥300 cells from 3 experiments. E) Quantification of spindle geometries following treatment with 10 μM STLC for 90 min without MG-132 treatment. Data represent the mean ± SEM; n≥280 cells from 3 experiments. F and G) Live imaging of HeLa and RPE-1 cell responses to STLC. Still images of HeLa (F) or RPE-1 (G) cells expressing mCherry-tubulin, arrested with 5 μM MG-132 for 100 min and then treated with 5 μM MG-132 and 10 μM STLC. Time is indicated in minutes and is relative to STLC addition. Scale bar, 5 μm.

explain this cell line variability. In all cell lines, more than 90% of mitotic cells contained monopolar spindles when treated with STLC for 90 min without MG-132 (n≥280; Figure 3.1E), demonstrating that they were susceptible to the drug. In addition, STLC displaced Eg5 from the spindle in cell lines which collapsed as well as those which maintained bipolarity without Eg5 (data not shown), further demonstrating susceptibility to the drug.

To verify that a high prevalence of monopolar spindles after MG-STLC treatment stemmed from bipolar spindle collapse rather than a failure to establish bipolarity, we monitored the STLC response of pre-assembled bipolar spindles by live cell imaging of fluorescent tubulin. After an MG-132 arrest and STLC treatment, bipolar spindles collapsed to monopoles in 17 out of 31 RPE-1 cells within one hour after STLC application (55%; Figure 3.1G); this may be lower than the percentage of monopoles in fixed-cells assays because a small number of cells may enter mitosis in STLC. In contrast to RPE-1 cells, a bipolar spindle collapsed to a monopole in only 1 out of 25 HeLa cells in the same time window (4%; Figure 3.1F). These results demonstrate that while Eg5 is required for the formation of bipolar spindles in all cell lines tested, it is dispensable for the maintenance of bipolar spindles in some but not all cell lines.

High K-MT stability correlates with bipolar spindle maintenance without Eg5

To understand the different abilities of human cell lines to maintain spindle bipolarity in the absence of Eg5 activity, we considered Kif15, the motor protein most necessary for bipolar spindle maintenance without Eg5 in HeLa and U2OS cells (Tanenbaum *et al.*, 2009; Vanneste *et al.*, 2009; Sturgill and Ohi, 2013). Kif15 is

expressed and localizes to the mitotic spindle in RPE-1 cells, suggesting that a lack of Kif15 cannot explain the sensitivity of RPE-1 cells to STLC at metaphase (Figure 3.6). Interestingly, Kif15 localizes specifically to K-MTs (Sturgill and Ohi, 2013), which are required for spindle bipolarity without Eg5 (Sturgill and Ohi, 2013). In addition, K-MT stability is known to vary among human cell lines. Non-transformed cell lines, including RPE-1, have less stable K-MTs than transformed cell lines, including U2OS (Bakhoum *et al.*, 2009a). Because Kif15 localizes to K-MTs and because K-MT stability is known to vary among human cell lines, we asked whether K-MT stability can explain the differences in the abilities of cell lines to maintain bipolarity without Eg5.

To assess the stability of K-MTs, we developed an assay using the tubulin-sequestering drug nocodazole. In cells treated with nocodazole for short time periods (a “nocodazole shock”), MTs that turn over rapidly disappear, but MTs that turn over slowly persist. We used nocodazole shock rather than fluorescence dissipation following photoactivation (FDAPA) (Zhai *et al.*, 1995; Bakhoum *et al.*, 2009a; Kabeche and Compton, 2013) for three reasons. First, although nocodazole shock does not report quantitative information on K-MT half-lives, it does provide enough temporal resolution to see reproducible differences across cell lines (Figure 3.2E). Furthermore, nocodazole shock allows for the rapid analysis of higher numbers of cells than FDAPA. Finally, counterstaining of kinetochores allows us to verify that the nocodazole-resistant polymer we see is derived from K-MTs instead of non-kinetochore-MTs (Figure 3.2, C and D), information that FDAPA cannot provide. We verified that nocodazole shock gives similar results to an established method by monitoring cold-stable MT levels. The

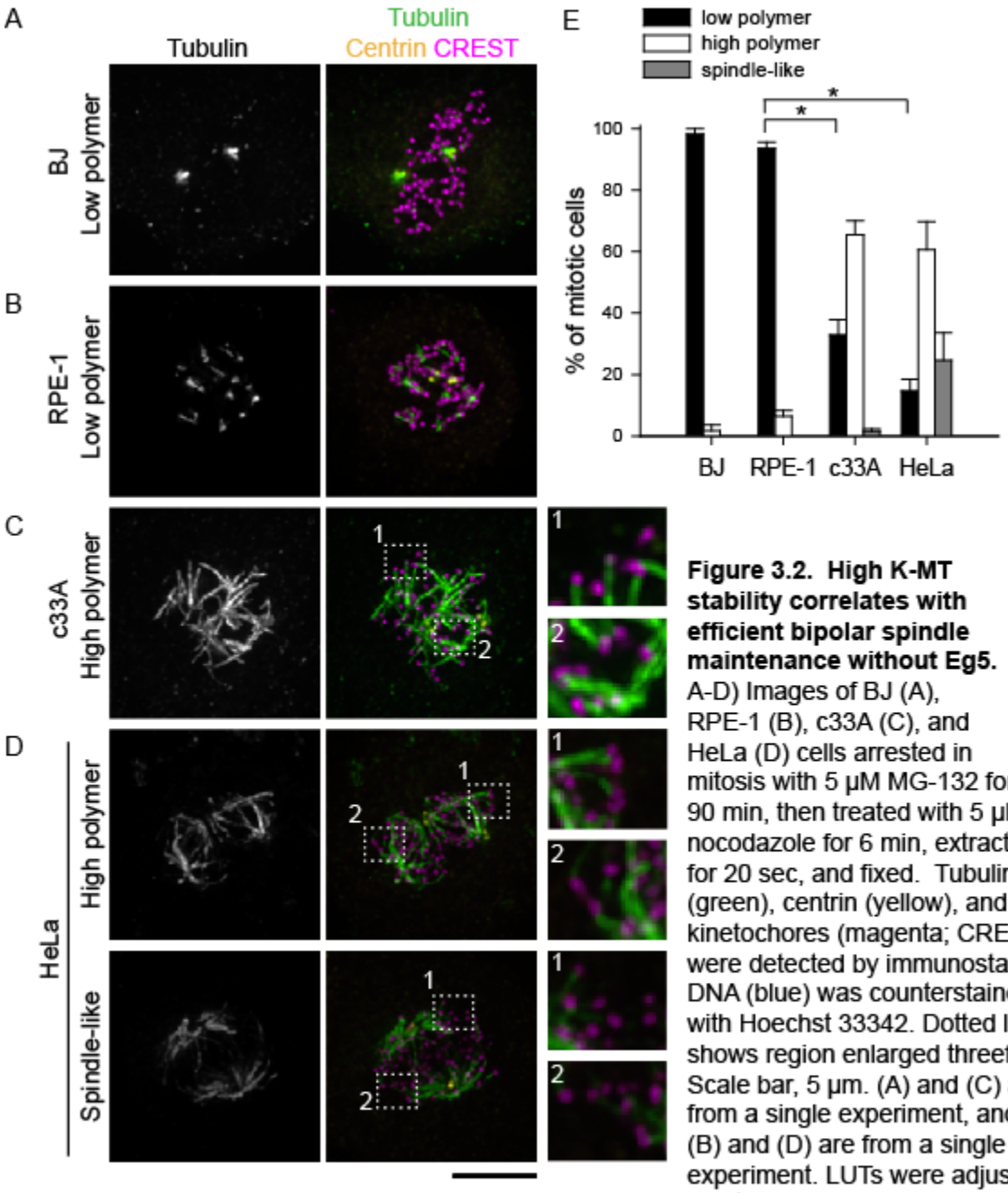

Figure 3.2. High K-MT stability correlates with efficient bipolar spindle maintenance without Eg5. A-D) Images of BJ (A), RPE-1 (B), c33A (C), and HeLa (D) cells arrested in mitosis with 5 μM MG-132 for 90 min, then treated with 5 μM nocodazole for 6 min, extracted for 20 sec, and fixed. Tubulin (green), centrin (yellow), and kinetochores (magenta; CREST) were detected by immunostaining. DNA (blue) was counterstained with Hoechst 33342. Dotted line shows region enlarged threefold. Scale bar, 5 μm. (A) and (C) are from a single experiment, and (B) and (D) are from a single experiment. LUTs were adjusted identically for images corresponding to the same experiment. E) Quantification of residual MT polymer levels following nocodazole treatment. Puncta or short streaks were scored as "low polymer;" long streaks joined at nodes were scored as "high polymer;" long streaks joined in two poles were scored as "spindle-like." Data represent the mean ± SEM; n≥100 cells from at least 3 experiments. *p<0.001.

K-MT stability trend revealed by cold temperatures matched the trend from nocodazole shock (data not shown). We continued with nocodazole shock because nocodazole is well characterized as a MT-specific agent, whereas prolonged cold temperatures are likely to affect other cell biochemical processes.

In accordance with published results (Bakhoum *et al.*, 2009a), we found that K-MTs in RPE-1 and BJ cells are unstable compared to those in HeLa or c33A cells (Figure 3.2). After a 6 min treatment with 5 μM nocodazole, nearly all RPE-1 and BJ cells had low levels of MT polymer (puncta or short MTs only; n≥100; Figure 3.2, A and B). In contrast, most HeLa and c33A cells had high levels of polymer; indeed, some cells retained a spindle-like structure with abundant K-MTs (n≥100; Figure 3.2, C and D). Therefore, among these four cell lines, the ability to efficiently maintain bipolarity without Eg5 correlates with high K-MT stability, consistent with the idea that K-MT stability impacts bipolar spindle maintenance without Eg5.

Destabilizing K-MTs Undermines Bipolar Spindle Maintenance in HeLa Cells

The model that cells with more stable K-MTs are better able to maintain bipolarity without Eg5 at metaphase makes two predictions: 1) destabilizing K-MTs would impair bipolar spindle maintenance, and 2) stabilizing K-MTs would promote bipolar spindle maintenance. To test the first prediction, we destabilized K-MTs in HeLa cells by depleting either of two K-MT stabilizing factors, HURP or Astrin (Figures 3.3B and 4B) (Sillje *et al.*, 2006; Manning *et al.*, 2010). Transfection of siRNAs targeting either HURP or Astrin decreased K-MT stability as gauged by the nocodazole shock assay (data not shown). Cells transfected in the same way were treated with MG-132 and STLC as in

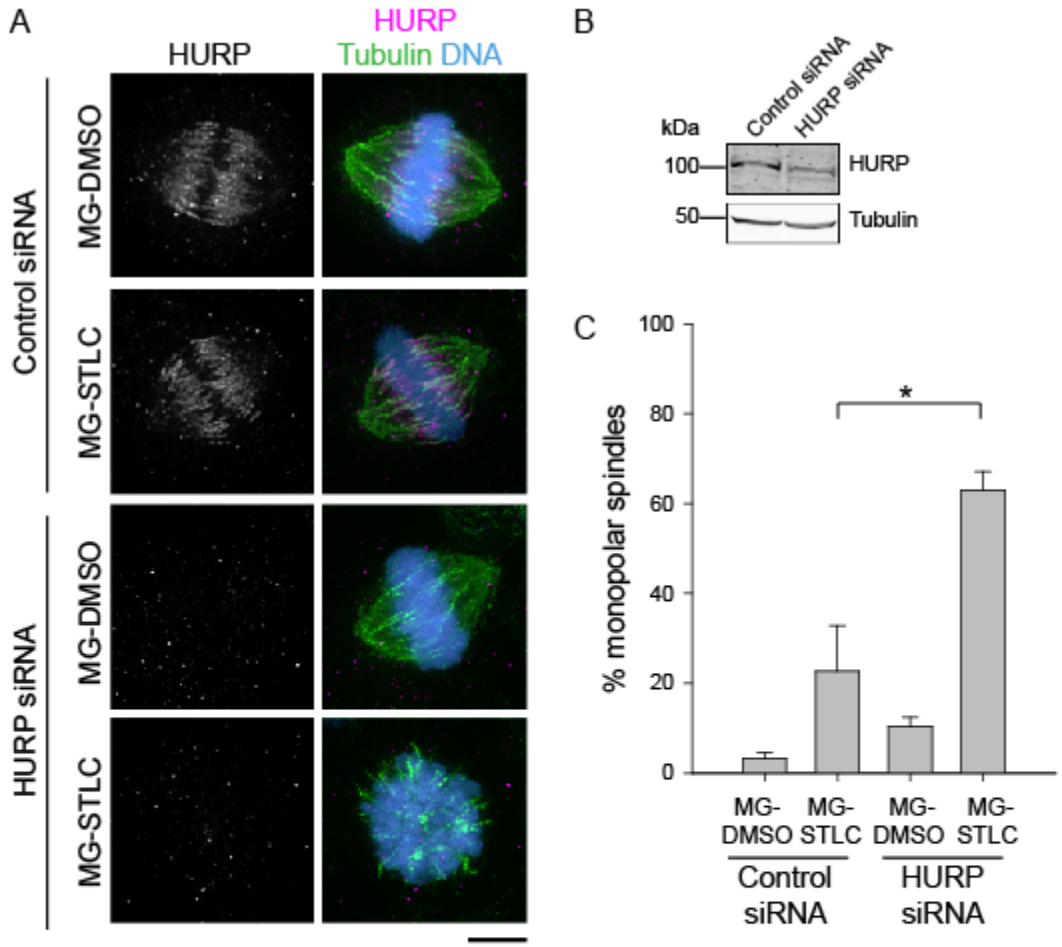

Figure 3.3. Depletion of HURP undermines bipolar spindle maintenance in HeLa cells following Eg5 inhibition. A) HURP depletion renders bipolar spindles in HeLa cells sensitive to Eg5 inhibition. HeLa cells transfected with control or HURP siRNA were treated with MG-DMSO or MG-STLC. Representative spindle geometries are shown. LUTs were scaled identically. Scale bar, 5 μm. B) Immunoblots of cell extracts prepared from cells depleted of HURP by siRNA transfection. To increase HURP signal, both control and HURP siRNA cells were treated with 5 μM MG-132 for 5h before lysis. Tubulin is shown as a loading control. C) Quantification of HeLa spindle geometries after treatment as in (A). Data represent the mean ± SEM; n≥300 cells from 3 experiments. *p<0.05.

Figure 3.1A. Depletion of HURP did not significantly alter spindle geometries in cells treated with MG-132 and DMSO (Figure 3.3, A and C). However, depletion of HURP and inhibition of Eg5 with STLC produced a strong increase in monopolar spindles (63.0±4.0%; n=300) compared to control siRNA cells (10.3±2.0%; n=300; Figure 3.3, A

and C). This result supports the idea that high K-MT stability is necessary for bipolar spindle maintenance without Eg5.

As previously reported (Thein *et al.*, 2007; Manning *et al.*, 2010), depletion of Astrin caused an increase in multipolar spindles (65.7±4.7%; n=300) compared to control siRNA cells (2.0±1.0%; n=300; Figure 3.4, A and C) in cells not treated with STLC. However, depletion of Astrin caused a strong increase in monopolar spindles following MG-STLC treatment (73.0±4.2%; n=300) compared to control siRNA cells (15.6±3.3%; n=300; Figure 3.4, A and C), in accordance with our results of HURP depletion. To test whether the multipolar spindles produced by Astrin depletion are predisposed to collapse to monopolar spindles without Eg5, we generated multipolar spindles by a different method and monitored their response to STLC treatment after an MG-132 arrest. We blocked cytokinesis in HeLa cells with the actin poison cytochalasin B, doubling both DNA content and centrosome number (Figure 3.4D). This treatment increased multipolar spindles without STLC, but did not increase the prevalence of monopolar spindles in cells treated with STLC, relative to cells not treated with cytochalasin B (Figure 3.4, D and E). This result suggests that in HeLa cells depleted of Astrin, it is the reduction of K-MT stability, not the generation of multipolar spindles, that drives the collapse to monopolar spindles without Eg5.

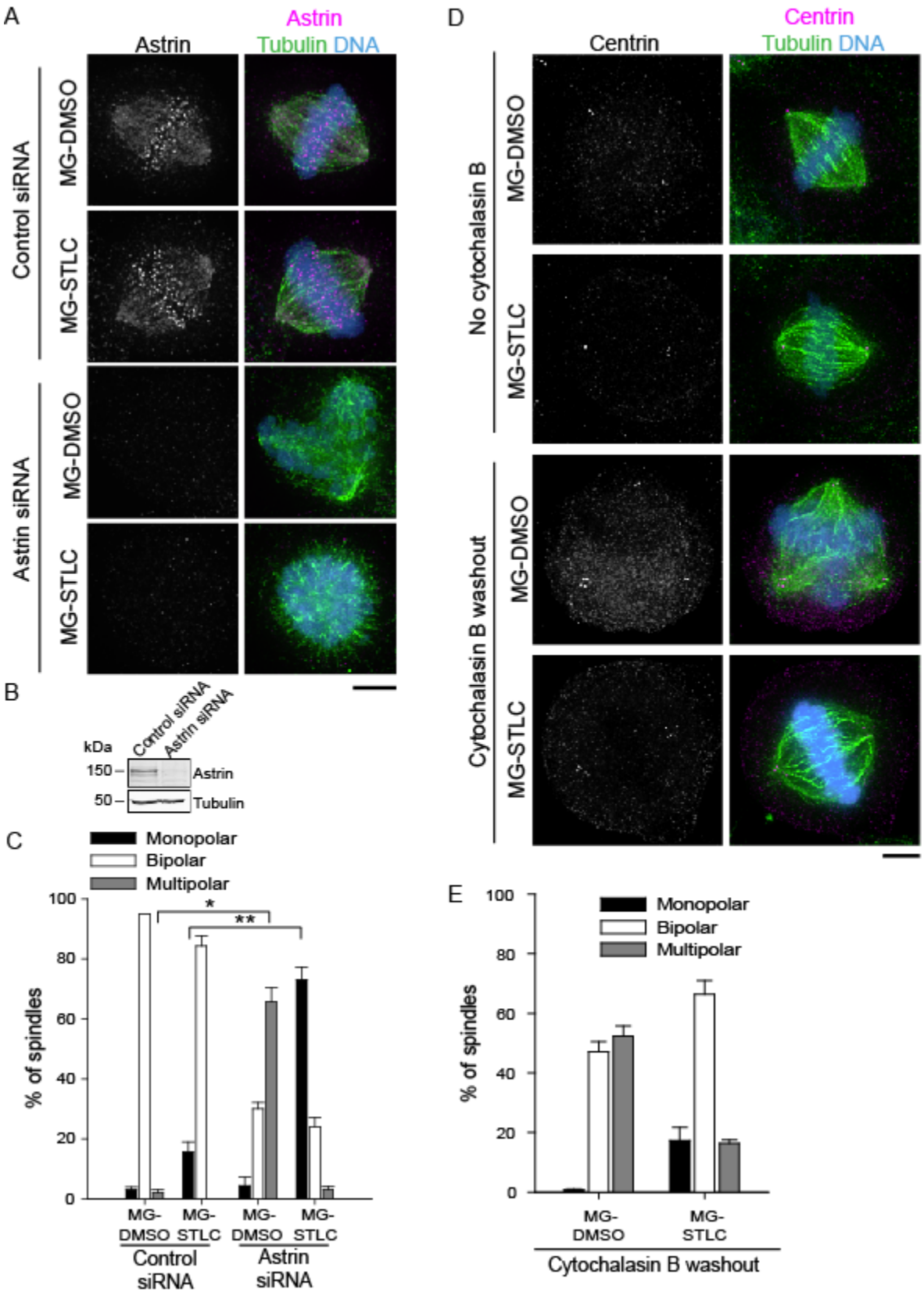

Figure 3.4 ***(legend next page)***

Stabilization of K-MTs promotes bipolar spindle maintenance in RPE-1 cells

To test the second prediction, we stabilized MTs in RPE-1 cells using a low concentration of taxol (2.5 nM). Taxol was applied at the start of the MG-132 arrest and was present through the STLC challenge (Figure 3.1A). 2.5 nM taxol did not cause gross changes in spindle geometry in DMSO-treated cells, but it strongly reduced the number of monopolar spindles following MG-STLC (23.9±6.2%; n=355) compared to non-taxol-treated cells (95.8±2.0%; n=330; Figure 3.5, A and B). We confirmed this finding in live cells by filming fluorescent tubulin. Spindles in 23 out of 25 MG-132-arrested RPE-1 cells treated with 2.5 nM taxol remained bipolar after one hour of STLC treatement (92%; Figure 3.5D). Importantly, the MT stability increase conferred by 2.5 nM taxol did not strongly interfere with mitotic progression. Differential interference contrast (DIC) microscopy of RPE-1 cells treated with 2.5 nM taxol showed that the time from nuclear envelope break-down to anaphase onset was slightly increased by the drug, but cells were nevertheless able to satisfy the spindle assembly checkpoint and exit mitosis (Figure 3.5C).

Figure 3.4. Depletion of Astrin undermines bipolar spindle maintenance in HeLa cells following Eg5 inhibition. A) Astrin depletion renders bipolar spindles in HeLa cells sensitive to Eg5 inhibition. HeLa cells transfected with control or Astrin siRNA were treated with MG-DMSO or MG-STLC. Representative spindle geometries are shown. LUTs were scaled identically. Scale bar, 5 µm. B) Immunoblots of cell extracts prepared from cells depleted of Astrin by siRNA transfection. Tubulin is shown as a loading control. C) Quantification of HeLa spindle geometries after treatment as in (A). Data represent the mean ± SEM; n≥300 cells from 3 experiments. *p<0.005. **p<0.001. D) Spindle multipolarity does not cause sensitivity to Eg5 inhibitors. HeLa cells were incubated in media with or without cytochalasin B for 24 h. 18 h after cytochalasin B washout, cells were treated with MG-DMSO or MG-STLC as in Fig. 1A. Representative images show centrosome duplication and resulting spindle geometries. LUTs were scaled identically. Scale bar, 5 µm. E) Quantification of HeLa spindle geometries after treatment as in (D). Data represent the mean ± SEM; n≥300 cells from 3 experiments.

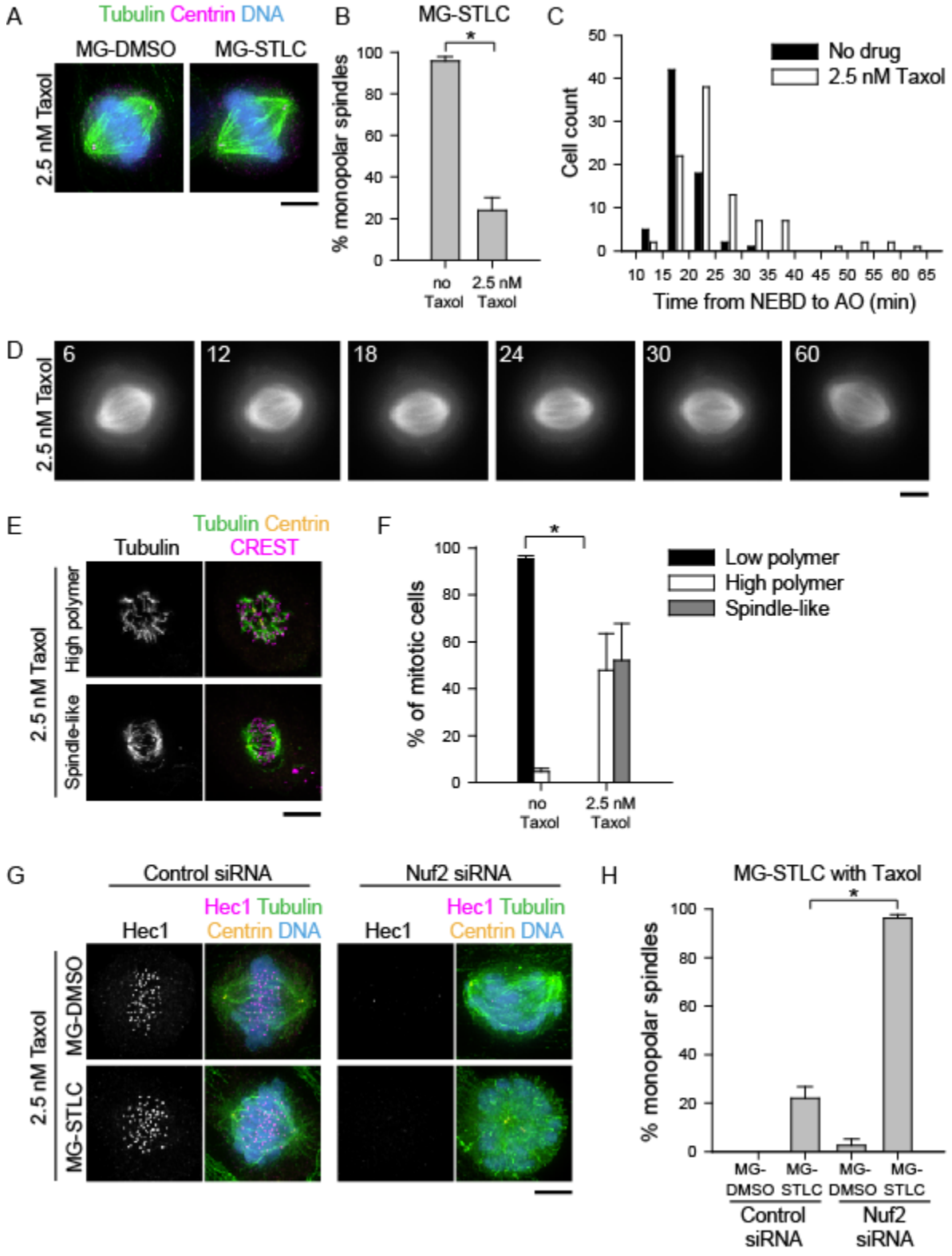

Figure 3.5 ***(legend next page)***

We confirmed that 2.5 nM taxol increased K-MT stability using nocodazole shock (Figure 3.5, E and F). In contrast to untreated RPE-1 cells (Figure 2), RPE-1 cells treated with 2.5 nM taxol had high polymer levels following nocodazole shock (Figure 3.5, E and F). To verify that taxol stabilized bipolarity through K-MTs, we blocked K-MT formation by depleting cells of the outer kinetochore component Nuf2 (DeLuca *et al.*, 2002), and treated them with MG-STLC or MG-DMSO in the presence of 2.5 nM taxol. In accordance with published results (DeLuca *et al.*, 2002), Nuf2 depletion produced bipolar spindles with a banana-shaped morphology and misaligned chromosomes (Figure 3.5G). Such cells were unable to maintain bipolarity with 2.5 nM taxol (96.2±1.5% monopolar; n=104; Figure 3.5, G and H), suggesting that stabilizing non-K-

Figure 3.5. Stabilization of K-MTs improves bipolar spindle maintenance in RPE-1 cells following Eg5 inhibition. A) Low concentrations of taxol prevent spindle collapse in RPE-1 cells exposed to STLC. Representative images of RPE-1 cells treated with 2.5 nM taxol plus MG-DMSO or MG-STLC as in Fig. 1A. Tubulin (green) and centrin (magenta) were detected by immunostaining. DNA (blue) was counterstained with Hoechst 33342. LUTs were scaled identically. Scale bar, 5 µm. B) Quantification of spindle geometries following MG-STLC treatment in RPE-1 cells treated with or without 2.5 nM Taxol. Data represent the mean ± SEM; n≥300 cells from 3 experiments. *p<0.001. C) 2.5 nM taxol does not prevent mitotic progression in RPE-1 cells. RPE-1 cells treated with or without 2.5 nM taxol were filmed by DIC, and the time from nuclear envelope breakdown (NEBD) to anaphase onset (AO) quantified. n≥68 cells from 2 experiments. D) Live cell imaging of an RPE-1 spindle challenged with STLC in the presence of 2.5 nM taxol. Still images of an RPE-1 cell expressing mCherry-tubulin treated first with 2.5 nM Taxol and 5 µM MG-132 for 100 min, and then treated with 2.5 nM Taxol, 5 µM MG-132, and 10 µM STLC. Time is indicated in minutes and is relative to STLC addition. Scale bar, 5 µm. E) 2.5 nM taxol promotes K-MT survival of nocodazole shock in RPE-1 cells. Representative images of RPE-1 cells treated with nocodazole as in Fig. 2 in the presence of 2.5 nM Taxol. Tubulin (green) and centrin (magenta) were detected by immunostaining. DNA (blue) was counterstained with Hoechst 33342. Scale bar, 5 µm. F) Quantification of residual MT polymer levels of RPE-1 cells with or without 2.5 nM Taxol following the nocodazole treatment as in (E). Data represent the mean ± SEM; n≥150 cells from 4 experiments. *p<0.001. G) The protective effect of low dose taxol to STLC is conferred through K-MTs. RPE-1 cells transfected with control or Nuf2 siRNA were treated with MG-DMSO or MG-STLC in the presence of 2.5 nM taxol. Representative spindle geometries are shown. LUTs are scaled identically. Scale bar, 5 µm. H) Quantification of spindle geometries after treatment as in (G). Data represent the mean ± SEM; n≥95 cells from 3 experiments. *p<0.005.

MTs is not sufficient to maintain bipolarity. This demonstrates that artificially increasing K-MT stability in RPE-1 cells enhances their ability to maintain spindle bipolarity without Eg5.

Perturbing K-MT stability influences bipolar spindle maintenance independently of Kif15 levels

Because Kif15 fails to bind the spindle in HeLa cells without K-MTs (Sturgill and Ohi, 2013), it is possible that our K-MT stability perturbations impact bipolar spindle maintenance by impacting Kif15 levels, rather than by having a direct effect on K-MT-generated forces. To examine this, we measured spindle-bound Kif15 fluorescence in HeLa cells depleted of HURP (Figure 3.6, A and B) and in RPE-1 cells treated with 2.5 nM taxol (Figure 3.6, C and D). Although each of these perturbations impacts the ability of cells to maintain spindle bipolarity without Eg5, neither perturbation changed the binding of Kif15 to the spindle. We therefore conclude that modulation of K-MT stability acts independently of Kif15 localization.

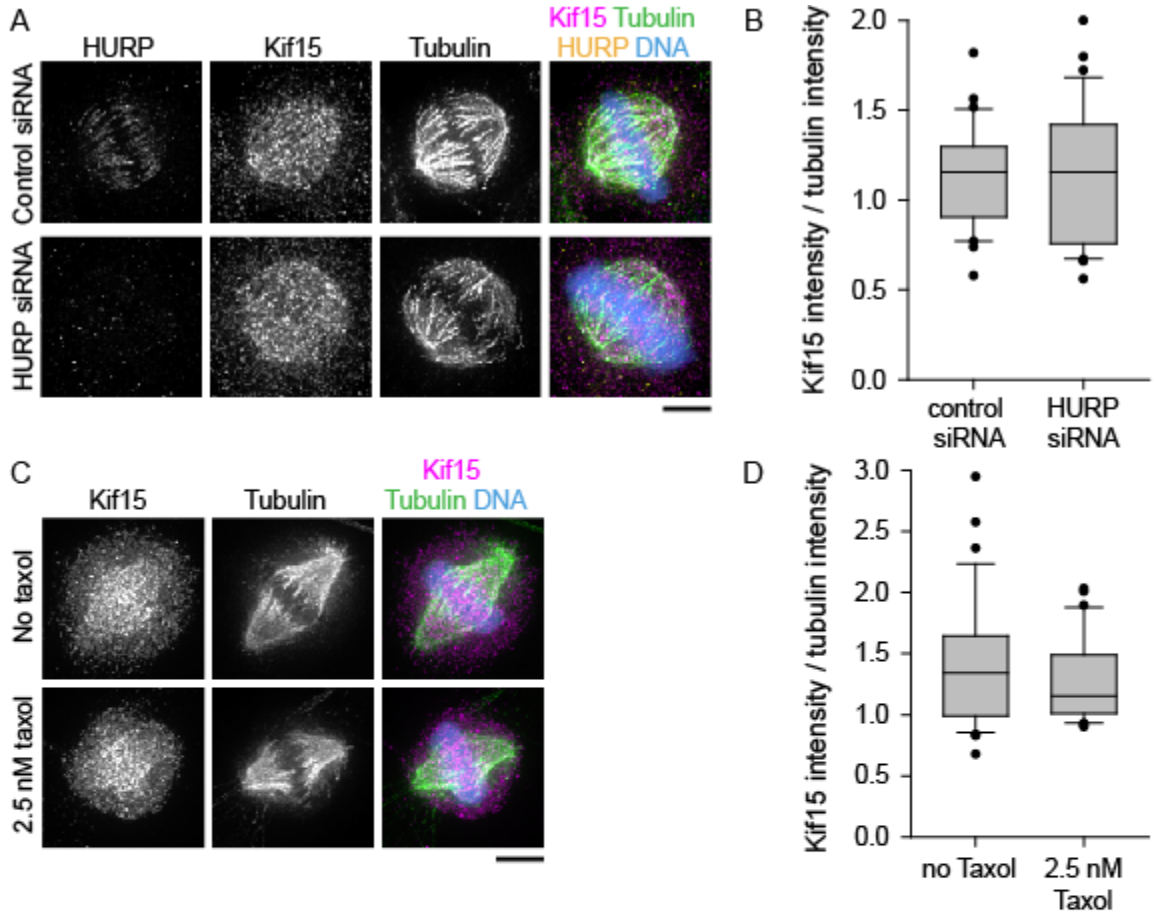

Figure 3.6. Kif15 spindle localization is independent of K-MT stability. A) Kif15 spindle localization is not reduced in HeLa cells depleted of HURP. HeLa cells transfected with control or HURP siRNA were treated with 5 μM MG-132 for 90 min. HURP (yellow), Kif15 (magenta), and tubulin (green) were detected by immunostaining. DNA (blue) was counterstained with Hoechst 33342. LUTs are scaled identically for each channel. Scale bar, 5 μm. B) Ratio of spindle Kif15 intensity to spindle tubulin intensity following treatment as in (A). Box-and-whisker plots display median flanked by 10th, 25th, 75th, and 90th percentiles. Each data set includes at least 30 cells from 3 experiments. p=0.86. C) Kif15 spindle localization is not increased in RPE-1 cells treated with 2.5 nM taxol. RPE-1 cells were treated with 5 μM MG-132 with or without 2.5 nM taxol for 90 min. Kif15 (magenta) and tubulin (green) were detected by immunostaining. DNA (blue) was counterstained with Hoechst 33342. LUTs are scaled identically for each channel. Scale bar, 5 μm. D) Ratio of spindle Kif15 intensity to spindle tubulin intensity following treatment as in (C). Box-and-whisker plots display median flanked by 10th, 25th, 75th, and 90th percentiles. Each data set includes at least 30 cells from 3 experiments. p=0.22.

Discussion

Force-balance, where sliding forces generated by molecular motors are balanced by oppositely directed motors or coupled to MT depolymerization, has provided a useful framework for understanding length control of the metaphase spindle (Goshima *et al.*, 2005). Kinesin-5 motors are central to this model and have been argued to act continuously throughout metaphase to antagonize inward-directed forces, generated by depolymerization of K-MTs (Goshima *et al.*, 2005) or motors of opposite directionality (Tanenbaum *et al.*, 2008). However, Eg5 is not required for bipolarity at metaphase in some vertebrate cell lines (Kollu *et al.*, 2009; Tanenbaum *et al.*, 2009; Vanneste *et al.*, 2009), indicating that other mechanisms must enforce bipolarity. Our findings highlight the potential importance of K-MTs in bipolarity maintenance. High K-MT stability correlated with the ability to maintain bipolarity without Eg5. Destabilizing K-MTs by depletion of HURP or Astrin impaired cells' ability to maintain bipolarity, while stabilizing K-MTs with low doses of taxol improved cells' ability to maintain bipolarity. Depletion of HURP or Astrin, or treatment with taxol, may produce complicated effects beyond merely stabilizing or destabilizing K-MTs; however, the most parsimonious interpretation of our results is that K-MT stability dictates the maintenance of K-MT stability without Eg5.

Our findings are consistent with two models (Figure 3.7). First, K-MTs may play an active role in spindle collapse, where depolymerization of unstable K-MT plus-ends generates significant inward-directed forces. In contrast, the plus-end depolymerization of stable K-MTs may not be sufficiently synchronized to generate inward-directed forces. This model is conceptually similar to the model proposed by Ganem and

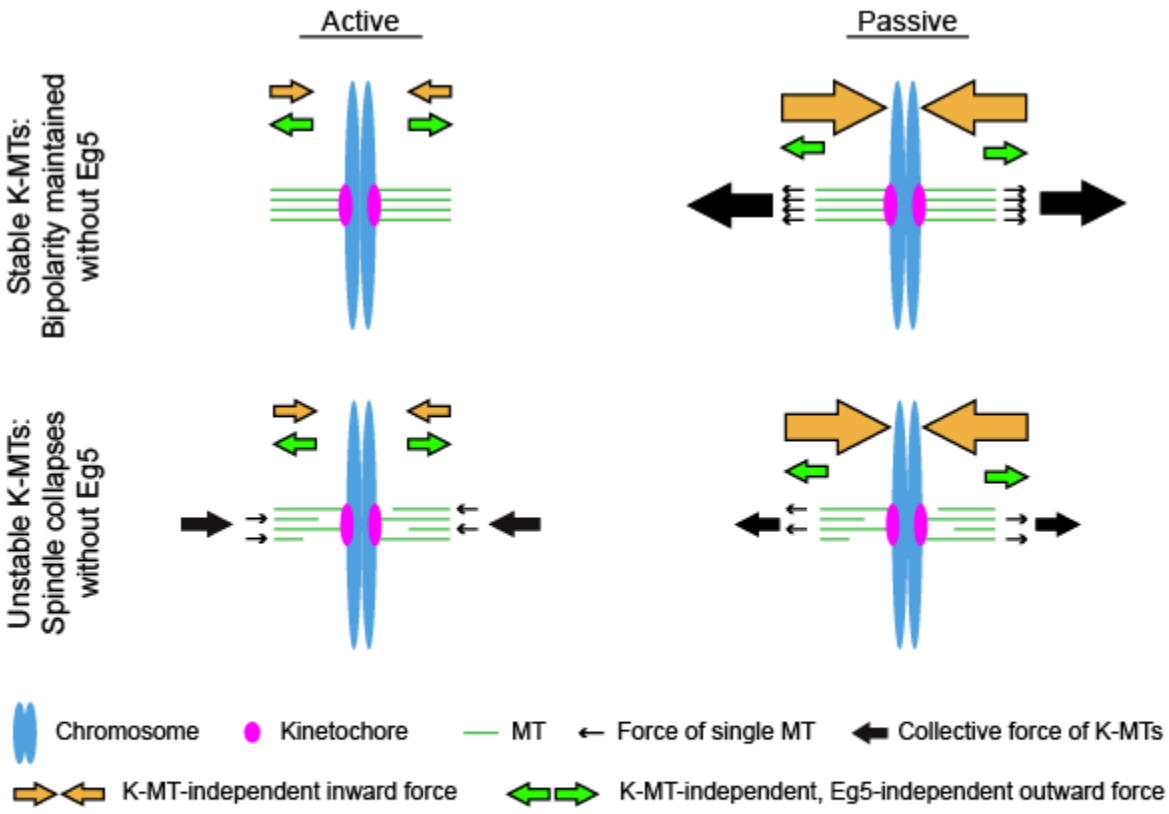

Figure 3.7. Model: K-MT stability determines the relative importance of Eg5 in maintaining spindle bipolarity. Cells with long-lived K-MTs (Top) do not continuously require Eg5, either because stable K-MTs do not pull on poles, or because stable K-MTs are competent to withstand stronger pulling forces. Cells with short-lived K-MTs (Bottom) continuously require Eg5, either because K-MT depolymerization pulls poles inward, or because unstable K-MTs cannot withstand pulling forces from other sources.

Compton, which proposed that unbalanced depolymerization of K-MT plus ends drives the formation of monopolar spindles (Ganem and Compton, 2004). However, this active, K-MT pulling model does not take into account the fact that spindles lacking K-MTs collapse without Eg5 (Fig 5H; Sturgill and Ohi, 2013), implying the existence of secondary inward-directed forces. Second, K-MTs may play a passive role during spindle maintenance, resisting collapse driven by other inward-directed forces, perhaps generated by minus end-directed motors (*ie.*, dynein and HSET). Stable K-MTs, organized into a long-lived, tightly packed bundle, would have great flexural rigidity (Felgner *et al.*, 1997) and thus be able to withstand inward forces generated by motors

of opposite directionality to Eg5. Importantly, this passive, outward force would be produced only when inward force was applied on the poles; therefore, it would not disrupt the steady-state length of the spindle with Eg5. Future work will be directed at discriminating between these possibilities.

The passive K-MT pushing model predicts that because the enforcement of bipolarity increases with decreasing K-MT turnover rates, it increases as a function of kinetochore occupancy by MTs. Unfortunately, existing methods to examine K-MT dynamics report only on MT turnover (Zhai et al., 1995; Bakhoum et al., 2009), not how long a single binding site is empty before it is filled by a regrowing MT. The best available readout for unoccupied K-MT binding sites is kinetochore localization of components of the spindle assembly checkpoint. These will not be useful to determine K-MT occupancy times at metaphase, however, because SAC components require multiple empty MT binding sites at a single kinetochore and several minutes of time before they are detectable (Dick and Gerlich, 2013). A binding site with a net "occupied" state, as K-MT binding sites are presumed to be at metaphase, will not generate a signal fast enough or strong enough to be detected. In the future, it will be important to measure the proportion of time a K-MT binding site is occupied, to understand how this timing impacts K-MT-generated forces.

In addition to HURP and Astrin, other proteins that act predominantly on K-MTs are known to stabilize the metaphase spindle in the absence of Eg5. Loss of Kif18A reduces K-MT stability (Manning *et al.*, 2010), and also renders bipolar spindles sensitive to Eg5 inhibitors (Tanenbaum *et al.*, 2009). These findings are consistent with our model that K-MT stability governs the requirement for Eg5 at metaphase. The

protein factor known to synergize most strongly with Eg5 in enforcing spindle bipolarity is Kif15 (Tanenbaum *et al.*, 2009; Vanneste *et al.*, 2009), a motor that decorates the K-MT lattice (Sturgill and Ohi, 2013; Vladimirou *et al.*, 2013). The biochemical properties of Kif15 central to this activity are not known, but because other K-MT stabilizing factors enforce bipolar spindle maintenance, our data suggest that the mechanism of Kif15 may also involve stabilization of K-MTs.

Our results suggest that maintenance of bipolarity is derived from spindle properties more complex than a purely motor-driven, push-pull mechanism. The architecture and dynamics of spindle MTs themselves may also be key. Meiotic spindles assembled in *Xenopus* egg extracts, for example, have a low proportion of K-MTs to short-lived non-K-MTs, and continuously require Eg5 to maintain bipolarity (Kapoor *et al.*, 2000). However, experimental elevation of the ratio of K-MTs to non-K-MTs causes spindles to become resistant to Eg5 inhibitors (Houghtaling *et al.*, 2009). Even in mitotic human cells, which are constructed from roughly equivalent amounts of non-K-MTs and K-MTs, the requirement for stable K-MTs to maintain bipolarity without Eg5 may not be universal. Although we have demonstrated that stable K-MTs promote bipolar spindle maintenance in HeLa and RPE-1 cells, other work has suggested that K-MTs are unnecessary for bipolar spindle maintenance without Eg5 in U2OS cells (Kollu *et al.*, 2009). Such phenotypic variation may be due to complex differences in genotype among transformed cells. Indeed, even cell lines with equivalently hyperstable K-MTs have varying levels of key mitotic proteins (Bakhoum *et al.*, 2009a). Importantly, however, our study shows that both non-transformed cell lines tested (RPE-1 and BJ) share the same response, suggesting that inefficient bipolar spindle maintenance

without Eg5 may be the prevailing phenotype among non-transformed human cells, and that bipolar spindle maintenance can be enhanced in these genetically normal cells by stabilizing K-MTs. One implication of our findings is that Eg5 inhibitors should not be used in combination with MT-stabilizing agents such as taxol, as such treatment regimens may impair rather than improve the killing of tumor cells.

CHAPTER 4

CDK-1 INHIBITION IN G2 STABILIZES KINETOCHORE-MICROTUBULES IN THE FOLLOWING MITOSIS

A. Sophia Gayek and Ryoma Ohi

Department of Cell and Developmental Biology, Vanderbilt University,

Nashville, TN 37232

A modified version has been submitted for publication as:

Gayek A.,S., Ohi R. CDK-1 inhibition in G2 stabilizes kinetochore-microtubules in the following mitosis.

CDK-1 inhibition in G2 promotes bipolarity maintenance without Eg5

In the course of our prior studies, we found that synchronizing RPE-1 cells at the G2/M transition using a CDK-1 inhibitor improved their ability to maintain bipolarity without Eg5. To understand this process more fully, we followed the drug regimen diagrammed in Figure 4.1A. We used a double thymidine block to arrest cells in S phase and released them from thymidine for five hours before incubating them with the highly specific and rapidly reversible CDK-1 inhibitor RO-3306 (Vassilev *et al.*, 2006). As a vehicle control for RO-3306, we incubated cells with an equivalent dilution of dimethyl sulfoxide (DMSO). After three hours in RO-3306 or DMSO, we extensively washed cells and used the MG-STLC assay described in Chapter 3 to monitor bipolarity maintenance: we applied the proteasome inhibitor MG-132 for 90 to block mitotic exit and allow cells time to build bipolar spindles, then added the Eg5 inhibitor S-trityl-L-cysteine (STLC) (DeBonis *et al.*, 2004) or DMSO as a vehicle control. To verify that STLC inhibited Eg5, we applied it to cells immediately after RO-3306 or DMSO washout as cells entered mitosis.

Inhibition of CDK-1 during G2 strongly improved the ability of cells to maintain the bipolarity of preformed spindles. The majority of RPE-1 cells treated with RO-3306 maintained bipolarity when treated with MG-132 then STLC, but most cells not treated with RO-3306 collapsed to form monopolar structures during the same drug treatments (Figure 4.1, B and C; DMSO, 75.7 ± 2.5% monpolar, mean ± standard error of the mean, n = 567; RO-3306, 33.3 ± 3.6% monopolar spindles, n=576). This effect cannot be due to a failure to build bipolar spindles: virtually no spindles were monopolar when cells were arrested with MG-132 without Eg5 inhibition, regardless of RO-3306

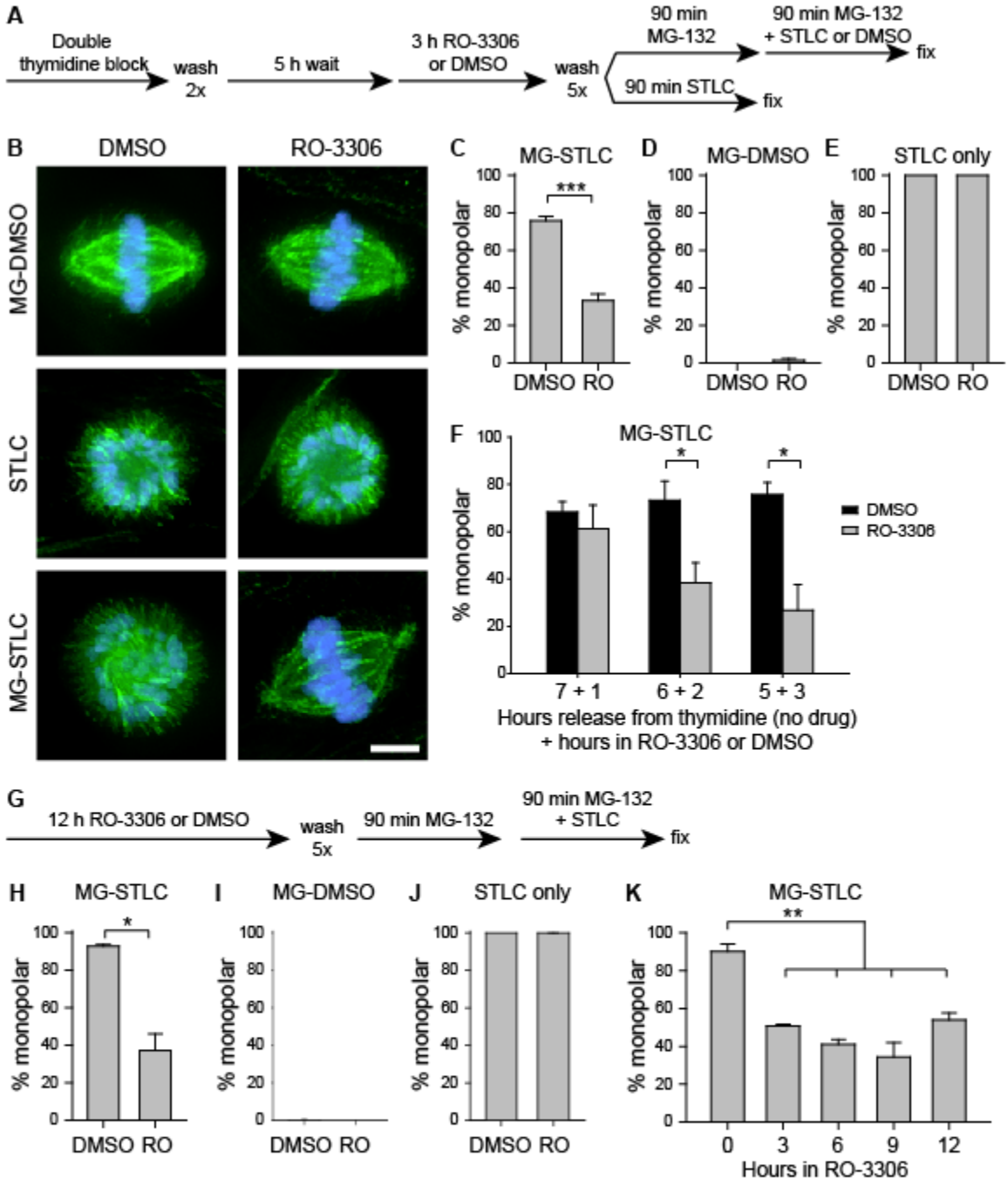

Figure 4.1. CDK-1 inhibition in G2 promotes bipolar spindle maintenance without Eg5 in RPE-1 cells. A) Schematic of drug treatments used in B-E. B) Representative images of spindles following drug treatments in (A). Tubulin is shown in green, and DNA is shown in blue. Scale bar, 5 µm. C-E) Quantification of the percentage of mitotic cells with monopolar spindles following MG-132 and STLC (C), MG-132 and DMSO (D), or STLC only (E) as diagrammed in (A). F) Quantification of the time dependence of the effect of RO-3306. Cells were treated as in (A), except that the length of time in media without drug and... *(continued next page)*

treatment (Figure 4.1, B and D; DMSO, 0% monopolar, n=300; RO-3306, 1.3 ± 0.9% monopolar, n=300). It also cannot be due to an inability of STLC to inhibit Eg5 in RO-3306-treated cells, since all spindles were monopolar when STLC was applied at mitotic entry, regardless of RO-3306 (Figure 4.1, B and E; DMSO, 100 ± 0% monopolar, n=300; RO-3306, 100 ± 0% monopolar, n=300).

To determine the time dependence of this effect, we varied the length of time that cells were treated with RO-3306. RO-3306 treatment for two or three hours gave equally strong effects, but shortening RO-3306 treatment to only one hour blocked its effect (Figure 4.1F; 3 h RO-3306, 29.8 ± 6.6% monopolar; 2 h RO-3306, 30.3 ± 8.4 % monopolar; 1 h RO-3306, 57.1 ± 9.8% monopolar; n≥357). This indicates that RO-3306 is acting through one of two time-dependent mechanisms: either the duration of CDK-1 inhibition matters and it must be over one hour, or the timing of CDK-1 inhibition matters and impacts a process that happens more than one hour before mitotic onset. Importantly, the lack of an effect at one hour rules out the possibility that the effect of RO-3306 was due to a failure to effectively wash out this drug.

To test whether the bipolarity-protective effect of CDK-1 inhibition requires pre-synchronization in S-phase, we treated cells directly with RO-3306, without an initial thymidine block (schematized in Figure 4.1G). Similarly to presynchronized cells, unsynchronized cells treated with RO-3306 before mitosis maintained bipolarity better

Figure 4.1 *(continued)* ...the length of time in RO-3306 were varied after thymidine washout. G) Schematic of drug treatments used in H-J. H-J) Quantification of the percentage of mitotic cells with monopolar spindles following MG-132 and STLC (H), MG-132 and DMSO (I), or STLC only (J) as diagrammed in (G). K) Quantification of the time dependence of the effect of RO-3306 without an initial thymidine block. Cells were treated as in (G), except that the length of time in RO-3306 was varied. For C-F and H-K, bars represent the mean and error bars represent the standard error of the mean (s.e.m.) of at least 300 cells from at least 3 experiments. * $p < 0.05$, ** $p < 0.01$, and *** $p < 0.001$ by a Students' t-test.

than control cells (Figure 4.1H; DMSO, 92.8 ± 0.9% monopolar; RO-3306, 37.3 ± 8.8% monopolar; n=600). CDK-1 inhibition during G2 had no impact on bipolarity when Eg5 was not inhibited (Figure 4.1I; DMSO, 0.3 ± 0.2% monopolar; RO-3306, 0% monopolar; n=600) or when Eg5 was inhibited as cells entered mitosis (Figure 4.1J; DMSO, 100% monopolar; RO-3306, 99.8 ± 0.2% monopolar; n=600). Increasing the duration of RO-3306 treatment from 3 to 12 h did not enhance its effect on bipolar spindle maintenance without Eg5 (Figure 4.1K; 3 h RO-3306, 50.7 ± 0.9% monopolar; 6 h RO-3306, 41.0 ± 2.5% monopolar; 9 h RO-3306, 34.3 ± 7.7% monopolar; 12 h RO-3306, 54.0 ± 3.6 % monopolar; n≥188).

The bipolarity-protective effect of CDK-1 inhibition in G2 depends on Kif15

As a first step in understanding the mechanism by which RO-3306 promotes bipolarity maintenance, we investigated its dependence on Kif15, the backup kinesin for Eg5. If RO-3306 increases the outward-directed forces that push the poles apart, then its effect should require Kif15; however, if RO-3306 decreases the inward-directed pulling on the poles by dynein or HSET, then RO-3306 treatment should still have an effect despite the loss of Kif15. We used RNAi to deplete Kif15 and started the double thymidine block one day after siRNA transfection to give a total of three days to knock down protein levels. The efficiency of Kif15 knockdown was highly variable across cells, so we immunostained our samples for Kif15 and only included cells with strongly reduced Kif15 in our analysis. We first scored bipolarity maintenance at a terminal time point (90 min Eg5 inhibition). We found that, while 3 h RO-3306 treatment improved bipolarity maintenance in control RNAi cells, spindles depleted of Kif15 uniformly

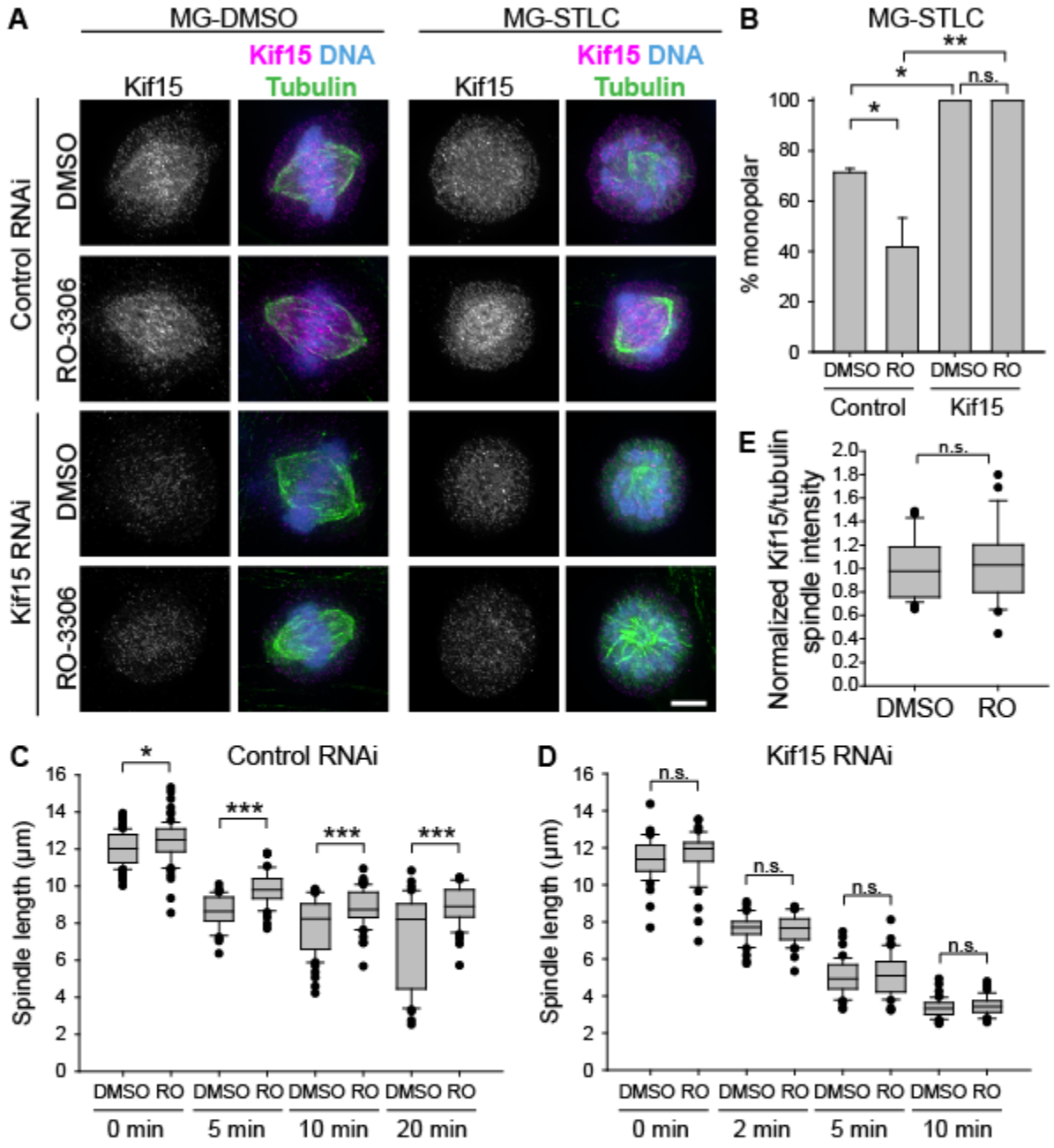

Figure 4.2. The bipolarity-protective effect of CDK-1 inhibition in G2 depends on Kif15.
A) Representative images of spindles following transfection with control or Kif15 siRNA, followed by the drug treatments described in Fig 1A. In overlay images, Kif15 is shown in magenta, tubulin is shown in green, and DNA is shown in blue. Scale bar, 5 µm.
B) Quantification of the percentage of mitotic cells with monopolar spindles following MG-STLC treatment as in (A). Bars represent the mean and error bars represent the standard error of the mean (s.e.m.) of at least 227 cells from 3 experiments.
C and D) Spindle lengths of collapsing cells transfected with control (C) or Kif15-specific siRNA (D), followed by the drug regimen described in 1A, and fixed at indicated time points after STLC application. Each bar represents at least 40 cells from at least 3 experiments.
(continued next page)

collapsed to monopolar structures, regardless of RO-3306 treatment (Figure 4.2, A and B; control siRNA, DMSO, 71.3 ± 0.9% monopolar; control siRNA, RO-3306, 41.7 ± 6.7% monopolar; Kif15 siRNA, DMSO, 100 ± 0% monopolar; Kif15 siRNA, RO-3306, 100 ± 0% monopolar; n≥227). We also monitored the apparent rate of spindle collapse by fixing cells at select time points after Eg5 inhibition and measuring their pole-to-pole spindle length. For these experiments, gamma-tubulin was used to precisely mark the locations of the spindle poles. We found that in cells transfected with control siRNA, RO-3306-treated cells had spindles that shortened more slowly than DMSO-treated cells (Figure 4.2C). In Kif15-depleted cells, however, any measurable effect of RO-3306 treatment was again abolished, and cells collapsed at indistinguishable rates regardless of RO-3306 pretreatment (Figure 4.2D). This indicates that CDK-1 inhibition is likely to impact Kif15 or a related pathway, rather than decreasing the inward force from dynein or HSET.

Since Kif15 is required for the protective effect that RO-3306 has on bipolarity maintenance, we used immunofluorescence to measure Kif15 levels relative to MTs in the spindle. We detected no difference in Kif15 levels or spindle binding in cells treated with RO-3306 or DMSO in G2 (Figure 4.2E; DMSO, 1.0 ± 0.0 A.U. normalized Kif15/tubulin; RO-3306, 1.0 ± 0.1 A.U. normalized Kif15/tubulin; n=29), suggesting that a related pathway, not Kif15 itself, is the mediator of RO-3306's bipolarity-protective effect. Since Kif15 localizes specifically to the K-MTs (Sturgill and Ohi, 2013), and

Figure 4.2 *(continued)* E) Normalized immunofluorescence intensity of Kif15 relative to MTs on the spindle for untransfected cells treated with a double thymidine block, washout, 5 h recovery, 3 h RO-3306 or DMSO, washout, and 90 min MG-132 before fixation. Each bar represents 29 cells from 3 experiments. For C-E, box-and-whisker plots indicate the 10th, 25th, 50th, 75th, and 90th percentile, as well as outliers. * $p < 0.05$, ** $p < 0.01$, *** $p < 0.001$, and n.s. (not significant) $p \geq 0.05$ by a Students' t-test.

since K-MT stability plays a role in enforcing spindle bipolarity (Chapter 3), we looked to see whether a change in K-MT stability might mediate RO-3306's bipolarity-protective effect.

CDK-1 inhibition in G2 increases K-MT stability

Because nanomolar concentrations of taxol improve bipolar spindle maintenance in RPE-1 cells (Chapter 3), we compared the effects of low-dose taxol to that of RO-3306, and also determined if dual drug treatments caused a synergistic increase in bipolarity maintenance. We found that treating cells with 0.5 nM taxol during mitosis without RO-3306 pretreatment improved bipolar spindle maintenance similarly to RO-3306 pretreatment without taxol (Figure 4.3A; DMSO, no Taxol, 77.8 ± 3.2% monopolar; RO-3306, no taxol, 32.0 ± 5.1% monopolar; DMSO, Taxol, 41.9 ± 3.6% monopolar; n≥827). Interestingly, the combination of RO-3306 treatment in G2 and 0.5 nM taxol during mitosis synergized to give a stronger effect than either alone (RO-3306, taxol, 4.3 ± 1.4% monopolar; n=900). This synergy could suggest either that the two perturbations act through separate pathways, or that the two work in the same pathway, but with a graded rather than switchlike impact on bipolar spindle maintenance.

To monitor K-MT stability, we used the nocodazole shock assay described in Chapter 3. We found that RO-3306 treatment in G2 stabilized K-MTs, causing a 1.7-fold increase in the average intensity of K-MT polymer remaining at 6 min (Figure 4.3 B and C; DMSO, 1.0 ± 0.0 AU sum intensity; RO-3306, 1.7 ± 0.1 AU sum intensity; n=75). This effect was only slightly smaller than the K-MT stabilization caused by 0.5 nM taxol

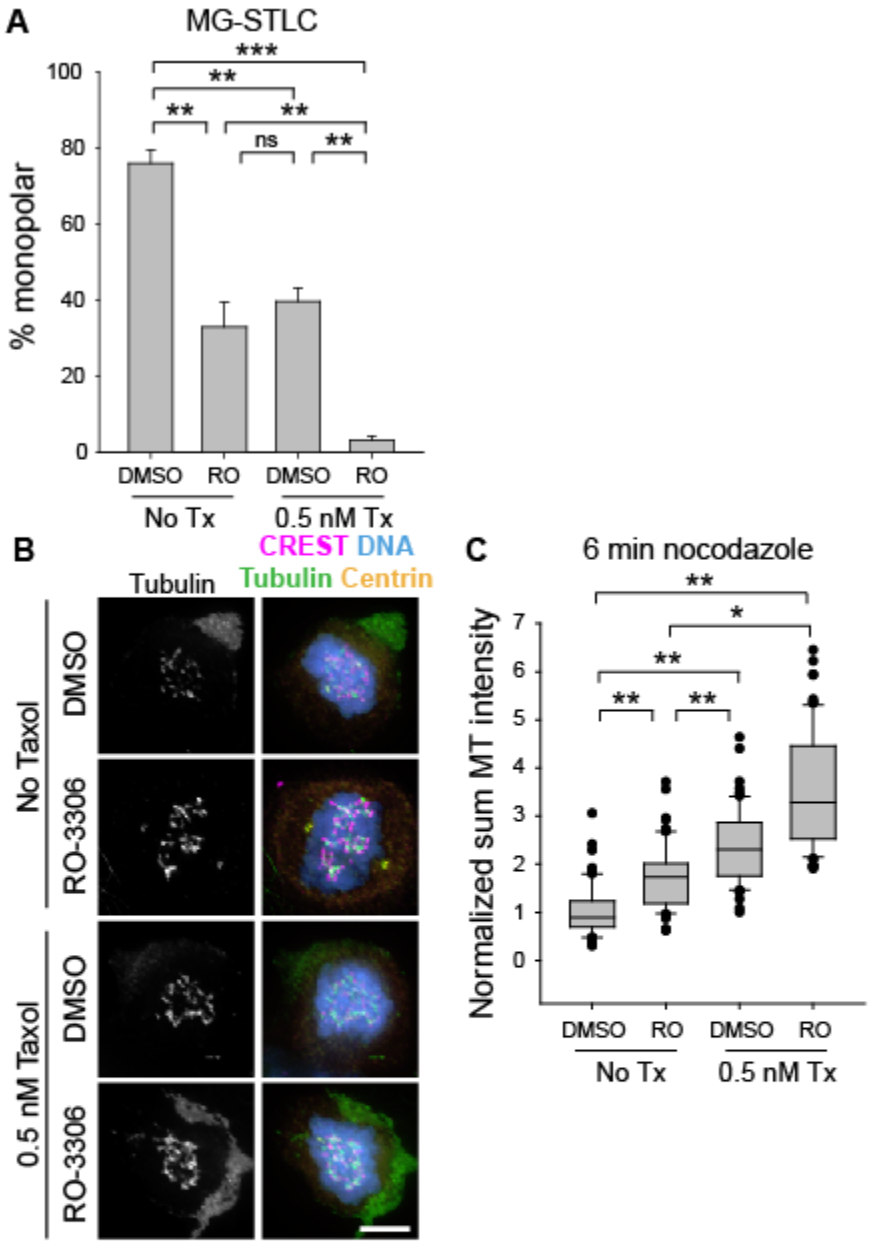

Figure 4.3. CDK-1 inhibition in G2 increases K-MT stability. A) Quantification of the percentage of mitotic cells with monopolar spindles following drug treatment as in 1A with or without the addition of 0.5 nM taxol during MG-132 and MG-132 + STLC. Bars represent the mean and error bars represent the s.e.m. of at least 827 cells from 5 experiments. B) Representative images of RPE-1 cells treated with a double thymidine block, washout, 5 h recovery, 3 h RO-3306 or DMSO, washout, 90 min MG-132 ± taxol, and 6 min NZ ± taxol. In overlay, tubulin is shown in green, kinetochores (CREST staining) in magenta, centrin in yellow, and DNA in blue; scale bar, 5 μm. C) Quantification of the sum fluorescence intensity of MT polymer remaining in cells after the treatments described in B, normalized to DMSO without taxol. Box-and-whisker plots indicate the 10th, 25th, 50th, 75th, and 90th percentile as well as outliers represents at least 60 cells from at least 4 experiments. * $p < 0.05$, ** $p < 0.01$, *** $p < 0.001$, and n.s. (not significant) $p \geq 0.05$ by a Students' t-test.

during mitosis (Figure 4.3 B and C; DMSO, taxol, 2.3 ± 0.1 A.U. sum intensity; n=60), indicating that the two perturbations may be promoting bipolar spindle maintenance through the same mechanism. Combination of RO-3306 in G2 and taxol in mitosis increased K-MT stability relative to either perturbation alone (Figure 4.3C; RO-3306, taxol, 3.5 ± 0.5 A.U. sum intensity; n=75), consistent with the idea that graded increases in K-MT stability lead to graded increases in the percentage of cells that can maintain bipolarity when Eg5 is inhibited.

High K-MT stability is required for CDK-1 inhibition in G2 to promote bipolarity maintenance

To test whether high K-MT stability is required for the bipolarity-protective effect of RO-3306, we reduced K-MT stability by depleting cells of HURP. As with Kif15, knockdown was inconsistent across the population of cells, so we analyzed only cells that showed no HURP signal by immunofluorescence (Figure 4.4A). We found that, while 3 h RO-3306 treatment before mitosis improved bipolar spindle maintenance in control-depleted cells, this effect was all but abolished in cells depleted of HURP (Figure 4.4, A and B; control siRNA, DMSO, 69.2 ± 4.7% monopolar; control siRNA, RO-3306, 42.5 ± 4.8% monopolar; HURP siRNA, DMSO, 100 ± 0% monopolar; HURP siRNA, RO-3306, 97.6 ± 1.0% monopolar; n≥61), suggesting that high K-MT stability is indeed required for RO-3306-induced bipolar spindle maintenance. To test whether artificially increasing K-MT stability could rescue the loss of K-MT stability from HURP depletion, we monitored bipolar spindle maintenance in HURP-depleted, taxol-treated cells. We found that HURP depletion strongly reduced the number of cells that could maintain

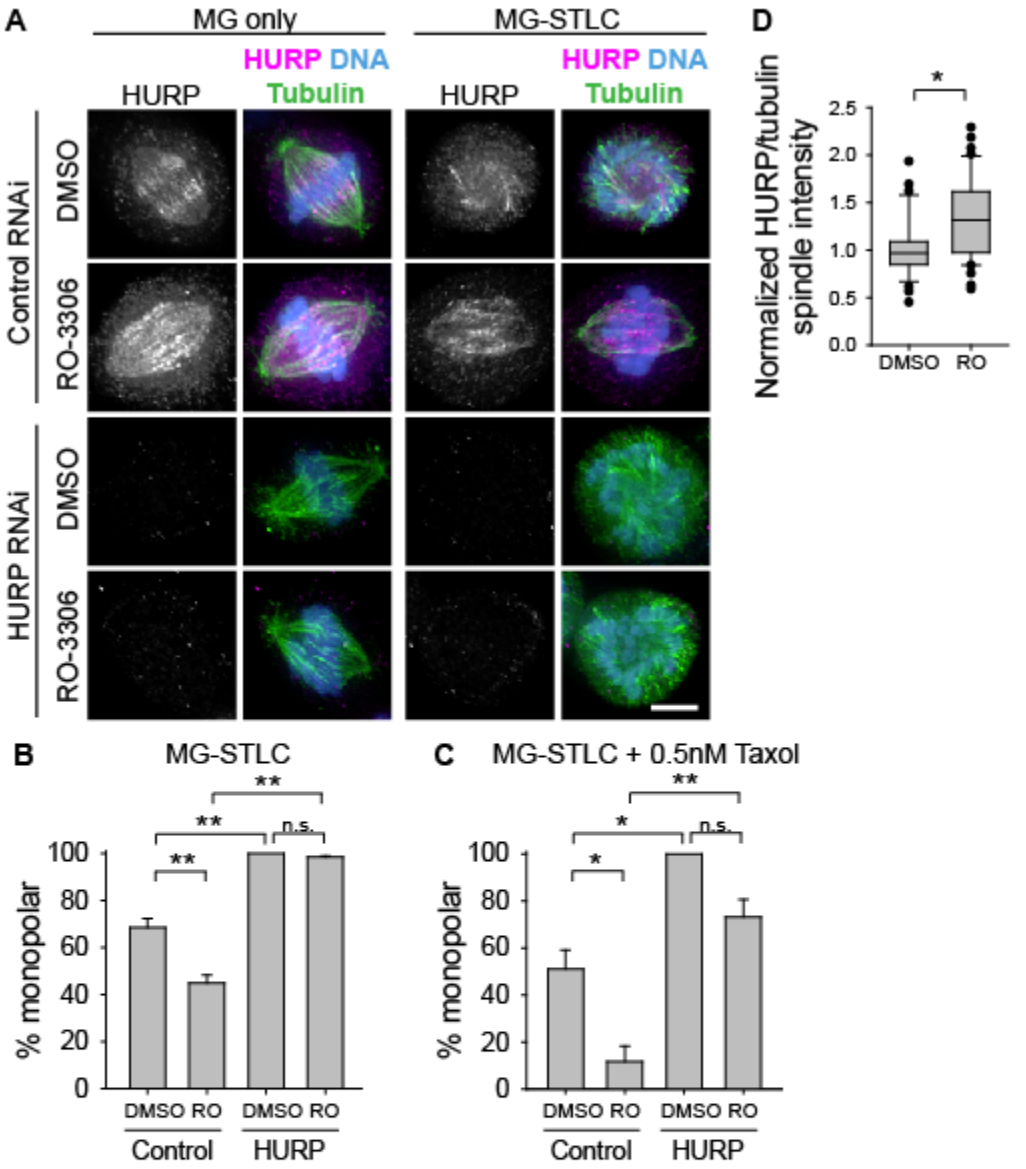

Figure 4.4. High K-MT stability is required for the bipolarity-protective effect of CDK-1 inhibition in G2. A) Representative images of spindles following transfection with control or HURP-targeting siRNA, followed by the drug treatments described in Fig 1A. In overlay images, HURP is shown in magenta, tubulin is shown in green, and DNA is shown in blue; scale bar, 5 μm. B and C) Quantification of the percentage of mitotic cells with monopolar spindles following MG-STLC treatment as in (A), without (E) or with (F) the inclusion of 0.5 nM taxol during MG-132 and MG-132 + STLC. Bars represent the mean and error bars represent the s.e.m. at least 34 cells from at least 3 experiments. D) Normalized immunofluorescence intensity of HURP relative to MTs on the spindle for untransfected cells treated with a double thymidine block, washout, 5 h recovery, 3 h RO-3306 or DMSO, washout, and 90 min MG-132 before fixation. Bars represent at least 39 cells from 4 experiments. Box-and-whisker plots indicate the 10th, 25th, 50th, 75th, and 90th percentile as well as outliers. * $p < 0.05$, ** $p < 0.01$, *** $p < 0.001$, and n.s. (not significant) $p \geq 0.05$ by a Students' t-test.

bipolarity under all drug conditions compared to control-depleted cells (Figure 4.4C); however, the combination of RO-3306 during G2 and 0.5 nM taxol during mitosis allowed for modest bipolar spindle maintenance despite depletion of HURP (HURP siRNA, RO-3306, taxol, 68.8 ± 10.4% monopolar; n=36). To test whether HURP itself might be impacted by RO-3306 treatment in G2, we used immunofluorescence to measure HURP levels relative to MTs in the spindle, and found a modest but significant increase in HURP spindle binding in cells treated with RO-3306 (Figure 4.4D; DMSO, 1.0 ± 0.0 A.U. normalized HURP/tubulin; RO-3306, 1.3 ± 0.1 A.U. normalized HURP/tubulin; n≥39). This indicates that, while HURP is not likely to be the sole mediator of the bipolarity-protective effect of RO-3306, it may be one factor leading to the increased K-MT stabilization and bipolarity protection.

CDK-1 inhibition in G2 increases the duration of mitosis and the frequency of mitotic errors

Since K-MT stability is closely tied to the accuracy of mitosis, we investigated whether RO-3306 might impact mitotic outcomes beyond bipolar spindle maintenance. First, we measured the time it took cells to complete mitosis, using nuclear envelope break down (NEBD) as a starting point and anaphase onset (AO) as an end point. We found that RO-3306 before mitosis increased the average time it took cells to complete mitosis, as well as increasing the variability in mitotic timing (Figure 4.5, A and B; DMSO, 20.7 ± 3.9 min; RO-3306, 28.6 ± 8.1 min; n≥116). This is consistent with the increase in the duration of mitosis seen with low-dose taxol in Chapter 3. Excessive K-MT stability can bias cells to form incorrect attachments between kinetochores and the

spindle, which lead to lagging chromosomes in anaphase (Cimini *et al.*, 2001) (Figure 4.5C). Lagging chromosomes are often segregated into micronuclei (Thompson and Compton, 2011), leading to their damage in the following cell cycle (Crasta *et al.*, 2012), and are indicative if not causative of high missegregation rates (Thompson and Compton, 2011). We found that RO-3306 treatment in G2 caused a 2.9-fold increase in lagging chromosomes in anaphase/telophase cells (Figure 4.5D; DMSO, 1.2 ± 0.8%; RO-3306, 5.7 ± 0.6%; n≥945), consistent with an increase in K-MT stability.

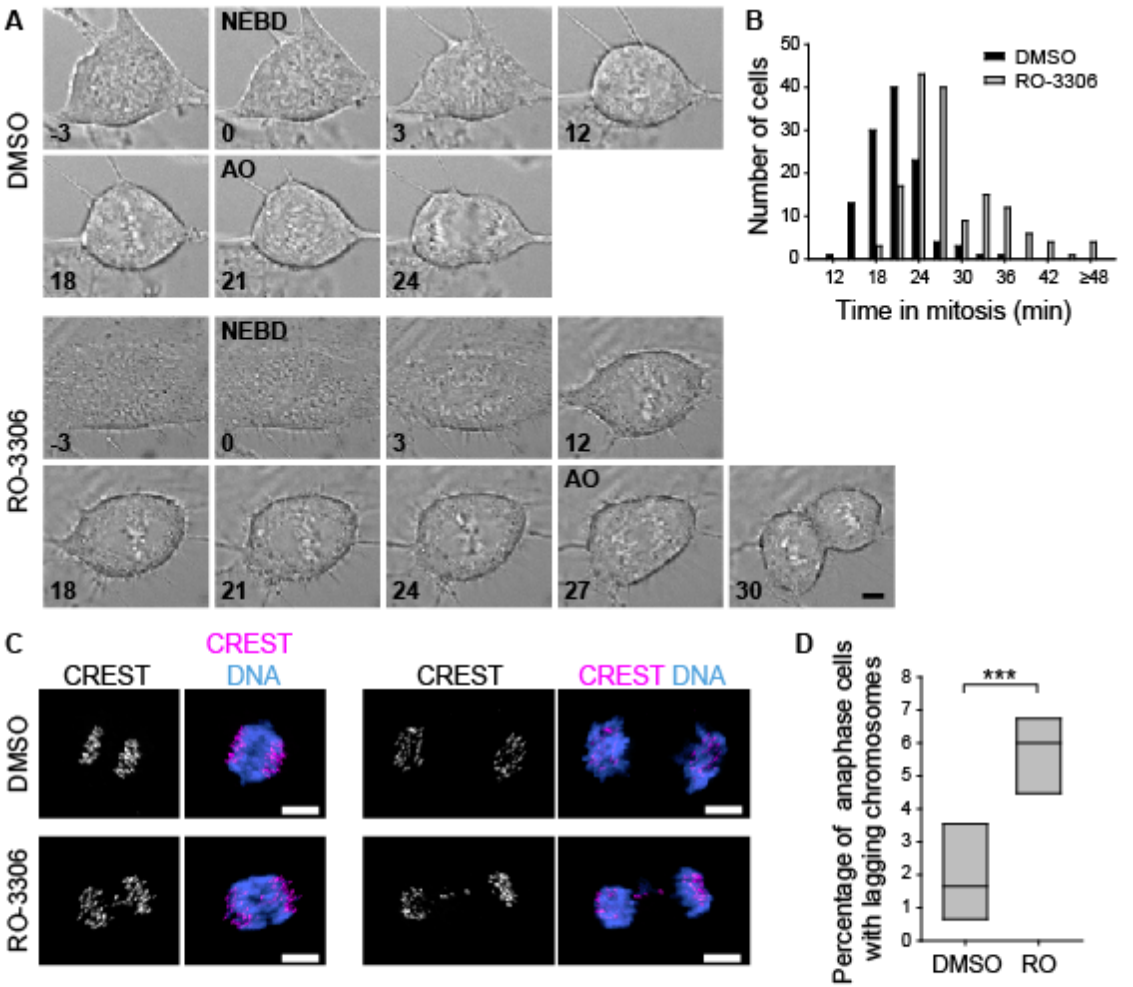

Figure 4.5. CDK-1 inhibition in G2 increases the duration of mitosis and the frequency of mitotic errors. A) Frames from DIC movies of representative cells undergoing mitosis following a double thymidine block, washout, 5 h recovery, 3 h RO-3306 or DMSO, and washout. The frames of nuclear envelope break down (NEBD) and anaphase onset (AO) are indicated; numbers indicate minutes from NEBD; scale bar, 5 µm. B) Histogram of the time from NEBD to AO in cells treated as in A. Each population includes at least 116 cells from 3 experiments. C) Illustrative images of cells treated as in A and fixed during early anaphase (left) or late anaphase/telophase (right). In overlays, kinetochores (CREST) are shown in magenta, and DNA is shown in blue. Although cells with lagging chromosomes were a minority population, they are shown to illustrate their morphology. LUTs were individually scaled for each image; scale bar, 5 µm. D) Quantification of the percentage of anaphase/telophase cells with lagging chromosomes following the treatments described in C. Box plot shows 25th, 50th, and 75th percentile from at least 945 cells from 4 experiments. *** $p < 0.001$ by a Students' t-test.

Discussion

In a simple view of the cell cycle, each stage may be independent of the stage before it: if a cell can clear a checkpoint to enter the next phase of the cycle, it must be ready to complete that next phase normally. However, lasting impacts of subtle cell cycle perturbations are now being characterized in subsequent stages of the cycle. For instance, prolonging prometaphase from its normal ~20 min to 90 min causes RPE-1 cells to undergo a p53-dependent arrest in the following G1 (Uetake and Sluder, 2010). Similarly, inhibiting cytokinesis with high doses of the actin-depolymerizing drug cytochalasin causes nontrasformed cells to arrest in the following G1 independently of cytokinesis failure itself (Uetake and Sluder, 2004). We have here characterized another example of cell cycle "memory": inhibition of CDK-1 in G2 increases K-MT stability in the subsequent mitosis.

It remains an open question how this memory is achieved. One possibility is that the flux of protein synthesis and degradation is disrupted in cells with CDK-1 inhibited. We know, for instance, that production of mitotic proteins continues during a prolonged G2 (Sherwood *et al.*, 1994), that CDK-1 primes some substrates for degradation by the proteasome (Hsu *et al.*, 2004), and that G2 cells kept in RO-3306 have different proteomic characteristics from undrugged G2 cells (Ly *et al.*, 2015). However, if disrupted protein production or degradation is responsible for stabilizing K-MTs, then cells must be very sensitive to the protein or proteins impacted, because RO-3306 treatment shows its full effect on bipolar spindle maintenance at 2-3 hours, with longer treatments not further improving bipolar spindle maintenance. A second possibility is that CDK-1 is active in very low levels in G2, and that this tiny activity is required for

normal K-MT stability. While FRET analysis indicated that CDK-1 only becomes highly active at the entry to mitosis (Gavet and Pines, 2010), some preparatory steps for mitosis, including Golgi fragmentation, occur hours in advance (Colanzi *et al.*, 2007), and one of these processes may impact K-MT stability. Finally, a third possibility is that washout of a CDK-1 inhibitor slightly disrupts normal kinetics of CDK-1 activation, even if they are switch-like, and these changed activation kinetics may impact K-MT stability. Further experiments will be required to distinguish between these possibilities.

We also do not know the precise effector or effectors that stabilize K-MTs following CDK-1 inhibition in G2. The increase in HURP binding to the spindle makes it a potential candidate, but the fact that RO-3306 synergizes with taxol even in HURP-depleted cells suggests that it may not be the only effector. It is possible that instead of a single K-MT stabilizing or destabilizing factor being strongly impacted, several such factors may be slightly impacted to give a large collective effect.

This work builds on our knowledge of how K-MT stability impacts bipolar spindle maintenance. In Chapter 3, we found that large differences in K-MT stability produced large differences in the ability to maintain bipolarity without Eg5, but we examined only drastic differences in K-MT stability. This prevented any interpretation about whether changes in K-MT stability lead to linear changes in bipolar spindle maintenance without Eg5, or whether they had nonlinear, thresholded effects on bipolar spindle maintenance. Here, we have found that much subtler increases in K-MT stability can strongly impact the ability of cells to maintain bipolarity. The fact that graded increases in K-MT stability produce graded increases in bipolar spindle maintenance without Eg5 suggest that one of two possibilities is true. First, it could be the case that a threshold stability of K-MTs

determines whether a spindle will collapse or maintain bipolarity without Eg5. However, such a threshold would have to be remarkably sharp to induce spindle collapse in only 30-40% of cells treated with RO-3306 in G2 or with 0.5 nM taxol in mitosis. Alternatively, it is more likely to be the case that increasing K-MT stability increases the likelihood of a spindle maintaining bipolarity without Eg5 in a graded manner in these mid-range levels of K-MT stability; at high and low extremes of K-MT stability, this would appear to be a threshold effect.

While the mechanism of K-MT stabilization is unknown, this work raises intriguing questions about the timing of CDK-1 activation and mitotic entry in undrugged cells. Cells may experience a prolonged G2 phase if either of two checkpoints is not satisfied. DNA damage will delay mitosis through the G2/M checkpoint, and tubulin poisons or other insults will delay or even reverse the early events of mitosis through the antephase checkpoint (Weinert and Hartwell, 1988; Rieder and Cole, 2000). It will be interesting to test whether transient activation of these checkpoints reproduces the phenotype of pharmacological CDK-1 inhibition in G2. On the other hand, since cells of the early embryo progress almost immediately from S phase to mitosis (Stead *et al.*, 2002), it will be interesting to see whether their K-MT attachments are any less stable than non-embryonic cells.

CHAPTER 5

CONCLUDING REMARKS

Here we have shown by several independent methods that elevating K-MT stability improves the ability of human mitotic spindles to maintain bipolarity in the absence of Eg5 activity. We have modulated K-MT stability using genetic perturbations (depletion of HURP and Astrin), pharmacolocical perturbations (low-dose taxol), and even used a previously unknown effect to stabilize K-MTs (inhibition of CDK-1 in G2). While none of these perturbations exclusively impacts K-MT stability, the fact that K-MT stability is the effect they share suggests that K-MT stability is responsible for their impact on bipolar spindle maintenance without Eg5. This finding, however, leaves open several questions for future work.

How does CDK-1 inhibition in G2 impact K-MT stability?

We have yet to understand the pathway that leads from CDK-1 inhibition in G2 to enhanced K-MT stability in the next mitosis. A disruption in protein homeostasis is one intriguing possibility: preventing cells from entering mitosis during CDK-1 inhibition could allow more time for the buildup of proteins translated in G2 and degraded at the end of mitosis. To learn whether overproduction of a G2-translated protein (or proteins) stabilizes K-MTs, it will be informative to carry out the drug regimen of Figure 4.1A using cycloheximide to attenuate protein synthesis during the RO-3306 block. If overproduction of a protein translated in G2 contributes to the effects of CDK-1

inhibition, then blocking or slowing translation should reduce the K-MT stabilization and improved bipolarity maintenance driven by RO-3306. Since cycloheximide may block mitotic entry by reducing the production of cyclin B, these experiments may need to be performed in the context of exogenous cyclin B overexpression. As a reverse method, we could apply low doses of a proteasome inhibitor like MG-132 to slow degradation of mitotic proteins translated in G2, and test whether this enhances K-MT stability and bipolarity maintenance independently of CDK-1 inhibition. Cycloheximide and MG-132 are blunt tools, however; a less invasive approach would be to use mass spectrometry to characterize the proteomes of cells treated with RO-3306 or DMSO after release from a thymidine block.

If a disruption in protein homeostasis lies at the hear of the K-MT stabilizing pathway, it would raise the possibility that extending the duration of G2 independently of direct CDK-1 inhibition could lead to similar K-MT stabilization. Given this possibility, it will be informative first to measure the duration of G2 in RPE-1 cells treated with RO-3306 or DMSO after a thymidine washout. If treatment with RO-3306 does prolong the G2 phase, we propose to test whether prolonging G2 by depolymerizing cells' MTs or damaging their DNA (to trigger the antephase or G2/M checkpoints, respectively) similarly increases K-MT stability. As the reciprocal experiment, we could test whether shortening G2 by treating cells with a Wee1 kinase inhibitor undermines the stability of their K-MTs and the ability of their spindles to maintain bipolarity when Eg5 is inhibited; however, we realize that forcing cells into mitosis prematurely may have other effects independent of G2 length and protein homeostasis.

An alternative hypothesis to the protein homeostasis model is that a low level of CDK-1 activity may be required in G2 in preparation for mitosis. In this case, slowing mitotic entry by triggering the antephase or G2/M checkpoints would be predicted to have no effect on K-MT stability and bipolarity maintenance. In addition, we might expect to detect a failure to carry out the preparatory steps in cells treated with RO-3306. For instance, visualizing the Golgi body may show that it is not properly distributed in RO-3306-treated G2 cells. However, a failure to see a defect in known G2 pathways which prepare for mitosis could not rule out that CDK-1 inhibition impacts an as-yet unknown pathway.

It will be worthwhile to determine the pathway that leads from CDK-1 inhibition in G2 to stabilization of K-MTs in mitosis because this represents an unknown form of cellular “memory” from one phase of the cell cycle to the next. If the duration of G2 disrupts protein homeostasis to impact the following mitosis, it may have interesting implications for more physiological cell cycles. For instance, if cells sense DNA damage in G2 and delay mitosis to correct it, do they then run an increased risk for missegregating a chromosome in anaphase? Does the precise length of G2 vary across cell types, whether comparing cells of different tissues, or comparing transformed to nontransformed cells or embryonic to adult cells? On the other hand, if a low level of CDK-1 activity in G2 is necessary to prepare for the next mitosis, how does the cell achieve a low level without activating the cascade that leads to full mitotic entry? These questions motivate additional investigation.

How does the stability of K-MTs enforce bipolar spindle maintenance?

The second key avenue for future work is in determining how high K-MT stability promotes bipolar spindle maintenance without Eg5. There are three main possibilities; while they are formally not mutually exclusive, we will consider them independently here. Two possibilities, that highly stable K-MTs sterically resist spindle collapse by providing an outward force, or that highly labile K-MTs pull the poles inward through repeated rounds of depolymerization, are outlined in Figure 3.7. However, an additional possibility is made clear by the results of Figure 4.2: that cells may require Kif15 to translate high K-MT stability into a greater ability to resist collapse.

There are several reasons why Kif15 may be necessary to see any bipolarity-protective effect from RO-3306 treatment in G2 that are independent of Kif15 being required to mediate the bipolarity-protective effect of high K-MT stability. First, because the K-MT stabilizing effects of RO-3306 treatment in G2 are relatively modest, a greater increase in K-MT stability (e.g., driven by 2.5 nM Taxol) may cause spindles to collapse more slowly compared to spindles with more labile K-MTs, despite an absence of Kif15. Second, Kif15 may promote K-MT stability, so its depletion may undermine the K-MT stability conferred by RO-3306. While untested, this idea is plausible because several kinesins are known to regulate MT dynamics, and a second K-MT localized motor, the Kinesin-8 Kif18A, stabilizes K-MTs (Manning *et al.*, 2010). It would be worth testing whether K-MTs are less stable in cells depleted of Kif15, or testing the impact of Kif15 on microtubule dynamics *in vitro*. Third, MT-intrinsic forces may be small relative to the motor-driven forces from Kif15, dynein, and HSET. If this were the case, the impact of

MT-intrinsic forces could be observed if motors were partially or fully depleted, as discussed in greater detail below.

These possibilities aside, the idea that Kif15 may mediate the effects of stable K-MTs warrants further investigation. We did not observe Kif15 binding to the spindle to change with changing K-MT stability (Figure 3.6), but steady-state localization to the spindle is a crude metric for Kif15 function. To look more closely for a link between high K-MT stability and increased Kif15 function, we could next measure the turnover rates of Kif15 on the spindle using FDAPA of a Kif15 construct tagged with a photoconvertible probe. Because Kif15 preferentially binds to MT bundles (Sturgill *et al.*, 2014), it may turn over more slowly on bundles of long-lived MTs rather than short-lived MTs, which may allow the production of greater motor-generated outward force in cells with hyperstable K-MTs. On the other hand, even if Kif15 turnover on the spindle is unchanged in response to changes in K-MT stability, MT sliding by Kif15 may still be greater on hyperstable K-MT substrates. *In vitro* experiments comparing Kif15-driven MT sliding of hyperstable MTs compared to more dynamic MTs may bring to light changes in force produced by Kif15 on bundles of different MT stabilities. While an inability to observe a difference in Kif15 localization, turnover, or sliding activity across different MT stability regimes would not rule out a role for Kif15 in translating high K-MT stability into improved bipolar spindle maintenance without Eg5, observing a difference in any of these experiments would suggest that Kif15 does play such a role.

Alternatively, Kif15 may slide MTs to push outward on the poles to the same degree irrespective of K-MT stability, and the dynamics of K-MTs themselves may provide force to resist or drive collapse. Several descriptive experiments may suggest

whether stable K-MTs push outward on the poles or whether labile K-MTs pull inward on the poles, although each experiment has caveats. First, it will be worthwhile to examine the distance between sister kinetochores of spindles in the process of collapse. If K-MTs are resisting collapse, the interkinetochore distance would be predicted to decrease, but if K-MT depolymerization is driving collapse, tension across pairs of sister kinetochores would be predicted to increase. However, local forces around the kinetochore may not reflect the global forces of the spindle, so the interkinetochore distance may not change as spindles collapse. Second, it may be informative to investigate the relationship between the number of kinetochores (therefore the number of K-MTs) and the rate of collapse. If K-MTs sterically resist collapse, then increasing their number should slow collapse, but if K-MT depolymerization reels the poles inward, then increasing their number should make spindles collapse faster; the opposite results would be expected for spindles with fewer kinetochores. Experimentally, K-MT number can be doubled by blocking cytokinesis using cytochalasin B as in Figure 3.4. However, this also doubles the number of centrosomes and the rest of the cell's contents, so a change in collapse rate could not be cleanly attributed to an increase in K-MT number. Alternatively, the number of kinetochores could be cut in half by inducing cells to undergo mitosis with an unreplicated genome, although this experiment also may have unpredictable effects on processes outside of K-MT number. As a cleaner approach, the number of kinetochores could be decreased by selective laser ablation of some kinetochores. An alternative method to decrease K-MT number (though not the number of kinetochores) would be to partially deplete Nuf2 from cells so that they can form some K-MT binding

sites, but fewer than normal cells. Determining whether these Nuf2 partial-depletion cells collapse faster or more slowly than their non-depleted counterparts could provide evidence for one of the models described in Chapter 3. However, all these experiments perturbing the number of K-MTs must be carefully controlled and monitored for their effects on Kif15, because disrupting K-MTs disrupts Kif15 localization to the spindle (Sturgill and Ohi, 2013). As a third approach to discriminating between stable K-MT pushing and labile K-MT pulling would be to weaken the link between sister kinetochores by depleting cohesin. Breaking this link would be predicted to disrupt force transmission through the kinetochore (therefore through K-MTs), so if cohesin-depleted cells collapse faster than non-depleted control cells, it would indicate that K-MTs may provide an outward force on the poles; the opposite would be true if cohesin-depleted cells collapsed more slowly than non-depleted controls.

Combinatorial depletion or inactivation of additional motor proteins besides Eg5 might also shed light on whether stable K-MTs push the poles outward or labile K-MTs pull them in. As explained above, K-MT-generated forces may be smaller than the forces produced by Kif15, dynein, and HSET across the entire range of physiological K-MT stabilities. If this is the case, then when Kif15 is depleted and Eg5 is inhibited, the large inward-directed forces from minus end-directed motors would mask the smaller effect of forces produced by K-MTs themselves. This explanation could be tested by using RNAi or small molecules to remove the activity of Eg5, Kif15, and dynein, then looking for an impact of K-MT stability on collapse or collapse rates. Removal of Eg5, Kif15, and dynein activity allows for bipolar spindle maintenance in U2OS cells, which have high K-MT stability (Bakhoum *et al.*, 2009a; van Heesbeen *et al.*, 2014). Carrying

out the same experiment in RPE-1 cells, or in HeLa cells depleted of HURP, may show bipolar spindle collapse if K-MT depolymerization pulls the poles inward, because cells with labile K-MTs would experience inward forces on the poles that U2OS cells lack because of the high stability of their K-MTs. However, if spindles without Eg5, Kif15, and dynein maintained bipolarity regardless of K-MT stability, it would suggest that K-MTs play a passive role in pushing the poles outward rather than actively pulling the poles together.

An independent line of investigation may shed additional light onto whether labile K-MTs pull the poles towards the kinetochores by their plus-end depolymerization. The Aurora B kinase phosphorylates substrates in the outer kinetochore, including Hec1, to promote kinetochore release from K-MTs (DeLuca *et al.*, 2011). As a result, if phosphorylation of Hec1 could be prevented, K-MTs would be less likely to be released from the kinetochore, leading to two effects. First, preventing Hec1 phosphorylation would be predicted to increase the stability of K-MTs, which would increase their capacity to produce outward force on the poles if they act as steric resistors to collapse. Second, preventing Hec1 phosphorylation would be predicted to allow each depolymerizing K-MT to maintain a longer connection with the kinetochore rather than breaking free, which would allow each depolymerizing K-MT to produce a greater inward force on the poles if K-MT depolymerization promotes collapse. By predicting opposite effects on bipolarity maintenance depending on whether K-MTs provide an outward or inward force on the poles, preventing Hec1 phosphorylation could be a means to disentangle these two hypotheses. Preventing Hec1 phosphorylation could be achieved by global knockdown or inhibition of Aurora B kinase, but this would be a

blunt approach because Aurora B has many substrates. Alternatively, Hec1 phosphorylation can be more specifically prevented by transfecting cells with a nonphosphorylatable mutant form of Hec1. Because of their potential for clean discrimination between the two hypotheses that K-MTs push outward or pull inward on the poles, these experiments are a priority for future work.

It is intriguing to consider that multipolar spindles tend to "collapse" to bipolar structures when Eg5 is inhibited (Figure 3.4). While this is consistent with the finding that splayed poles tend to coalesce into tighter poles when Eg5 is inhibited (van Heesbeen *et al.*, 2014), it is not immediately obvious how the residual outward-directed forces generated by Kif15 (and perhaps K-MTs) would promote pole separation only along a single axis rather than along the multiple axes of multipolar spindles. It will be informative to visualize live the process of multipolar spindles "collapsing" to form bipolar spindles, to determine whether this "collapse" has the same characteristics as the collapse of bipolar spindles to monopolar structures.

Although modern biology often idealizes identifying single molecules responsible for a given effect, the modulation of K-MT stability studied here is truly a systems-level problem, not likely to governed by a single molecule or small set of molecules. While this might be guessed by the sheer number of factors that regulate K-MT attachment and stability, it is underscored by the fact that loss of one K-MT stabilizing factor (HURP) can be partially rescued by stabilization of K-MTs by other means (CDK-1 inhibition and taxol; Figure 4.4). This suggests that a single molecular mechanism for K-MT stabilization is not critical for bipolar spindle maintenance; rather, the net effect of K-MT stability by many factors is what is likely to influence the maintenance of

bipolarity. This hypothesis could be tested by extending the experiments of Figure 4.4 to include depletion of other K-MT stabilizing factors, and rescue by overexpression of other K-MT-stabilizing factors or a broader range of Taxol doses. If depletion of one K-MT stabilizing factor can be rescued either by overexpression of another protein or by the application of a low dose of Taxol, it would underscore the interchangeability of K-MT stabilizing factors in the pathway that leads to bipolar spindle maintenance without Eg5.

Further experiments will be required to determine whether high K-MT stability allows for greater Kif15 activity, whether high K-MT stability leads to steric outward forces on the poles, or whether low K-MT stability provides inward force to pull the poles inward. Because of the weight of data demonstrating that K-MTs exert pulling forces on the kinetochore in the course of normal mitoses, I favor the model that labile K-MTs pull the poles inward; however, experiments in the Ohi laboratory are still ongoing to determine whether this is the true explanation. Since it lies at the intersection between two processes critical for successful mitosis, it will be valuable to continue work to determine the mechanism by which highly stable K-MTs enforce the maintenance of mitotic spindle bipolarity.

REFERENCES

Akiyoshi, B., Sarangapani, K.K., Powers, A.F., Nelson, C.R., Reichow, S.L., Arellano-Santoyo, H., Gonen, T., Ranish, J.A., Asbury, C.L., and Biggins, S. (2010). Tension directly stabilizes reconstituted kinetochore-microtubule attachments. Nature *468*, 576-579.

Amos, L., and Klug, A. (1974). Arrangement of subunits in flagellar microtubules. J Cell Sci *14*, 523-549.

Bakhoum, S.F., Genovese, G., and Compton, D.A. (2009a). Deviant kinetochore microtubule dynamics underlie chromosomal instability. Curr Biol *19*, 1937-1942.

Bakhoum, S.F., Thompson, S.L., Manning, A.L., and Compton, D.A. (2009b). Genome stability is ensured by temporal control of kinetochore-microtubule dynamics. Nat Cell Biol *11*, 27-35.

Bell, J.C., and Straight, A.F. (2015). Condensing chromosome condensation. Nat Cell Biol *17*, 964-965.

Belmont, L.D., Hyman, A.A., Sawin, K.E., and Mitchison, T.J. (1990). Real-time visualization of cell cycle-dependent changes in microtubule dynamics in cytoplasmic extracts. Cell *62*, 579-589.

Bishop, J.D., Han, Z., and Schumacher, J.M. (2005). The Caenorhabditis elegans Aurora B kinase AIR-2 phosphorylates and is required for the localization of a BimC kinesin to meiotic and mitotic spindles. Mol Biol Cell *16*, 742-756.

Blangy, A., Lane, H.A., d'Herin, P., Harper, M., Kress, M., and Nigg, E.A. (1995). Phosphorylation by p34cdc2 regulates spindle association of human Eg5, a kinesin-related motor essential for bipolar spindle formation in vivo. Cell *83*, 1159-1169.

Bloom, J., and Cross, F.R. (2007). Multiple levels of cyclin specificity in cell-cycle control. Nat Rev Mol Cell Biol *8*, 149-160.

Brinkley, B.R., and Cartwright, J., Jr. (1975). Cold-labile and cold-stable microtubules in the mitotic spindle of mammalian cells. Ann N Y Acad Sci *253*, 428-439.

Brugues, J., Nuzzo, V., Mazur, E., and Needleman, D.J. (2012). Nucleation and transport organize microtubules in metaphase spindles. Cell *149*, 554-564.

Burbank, K.S., Groen, A.C., Perlman, Z.E., Fisher, D.S., and Mitchison, T.J. (2006). A new method reveals microtubule minus ends throughout the meiotic spindle. J Cell Biol *175*, 369-375.

Cai, S., Weaver, L.N., Ems-McClung, S.C., and Walczak, C.E. (2009). Kinesin-14 family proteins HSET/XCTK2 control spindle length by cross-linking and sliding microtubules. Mol Biol Cell *20*, 1348-1359.

Cameron, L.A., Yang, G., Cimini, D., Canman, J.C., Kisurina-Evgenieva, O., Khodjakov, A., Danuser, G., and Salmon, E.D. (2006). Kinesin 5-independent poleward flux of kinetochore microtubules in PtK1 cells. J Cell Biol *173*, 173-179.

Cassimeris, L., Pryer, N.K., and Salmon, E.D. (1988). Real-time observations of microtubule dynamic instability in living cells. J Cell Biol *107*, 2223-2231.

Cheeseman, I.M. (2014). The kinetochore. Cold Spring Harb Perspect Biol *6*, a015826.

Choi, S.H., and McCollum, D. (2012). A role for metaphase spindle elongation forces in correction of merotelic kinetochore attachments. Curr Biol *22*, 225-230.

Cimini, D., Howell, B., Maddox, P., Khodjakov, A., Degrassi, F., and Salmon, E.D. (2001). Merotelic kinetochore orientation is a major mechanism of aneuploidy in mitotic mammalian tissue cells. J Cell Biol *153*, 517-527.

Cimini, D., Wan, X., Hirel, C.B., and Salmon, E.D. (2006). Aurora kinase promotes turnover of kinetochore microtubules to reduce chromosome segregation errors. Curr Biol *16*, 1711-1718.

Colanzi, A., Hidalgo Carcedo, C., Persico, A., Cericola, C., Turacchio, G., Bonazzi, M., Luini, A., and Corda, D. (2007). The Golgi mitotic checkpoint is controlled by BARS-dependent fission of the Golgi ribbon into separate stacks in G2. EMBO J *26*, 2465-2476.

Crasta, K., Ganem, N.J., Dagher, R., Lantermann, A.B., Ivanova, E.V., Pan, Y., Nezi, L., Protopopov, A., Chowdhury, D., and Pellman, D. (2012). DNA breaks and chromosome pulverization from errors in mitosis. Nature *482*, 53-58.

DeBonis, S., Skoufias, D.A., Lebeau, L., Lopez, R., Robin, G., Margolis, R.L., Wade, R.H., and Kozielski, F. (2004). In vitro screening for inhibitors of the human mitotic kinesin Eg5 with antimitotic and antitumor activities. Mol Cancer Ther *3*, 1079-1090.

DeLuca, J.G., Moree, B., Hickey, J.M., Kilmartin, J.V., and Salmon, E.D. (2002). hNuf2 inhibition blocks stable kinetochore-microtubule attachment and induces mitotic cell death in HeLa cells. J Cell Biol *159*, 549-555.

DeLuca, K.F., Lens, S.M., and DeLuca, J.G. (2011). Temporal changes in Hec1 phosphorylation control kinetochore-microtubule attachment stability during mitosis. J Cell Sci *124*, 622-634.

Desai, A., Verma, S., Mitchison, T.J., and Walczak, C.E. (1999). Kin I kinesins are microtubule-destabilizing enzymes. Cell *96*, 69-78.

Ding, R., McDonald, K.L., and McIntosh, J.R. (1993). Three-dimensional reconstruction and analysis of mitotic spindles from the yeast, Schizosaccharomyces pombe. J Cell Biol *120*, 141-151.

Dogterom, M., and Yurke, B. (1997). Measurement of the force-velocity relation for growing microtubules. Science *278*, 856-860.

Dong, Y., Vanden Beldt, K.J., Meng, X., Khodjakov, A., and McEwen, B.F. (2007). The outer plate in vertebrate kinetochores is a flexible network with multiple microtubule interactions. Nat Cell Biol *9*, 516-522.

Drosopoulos, K., Tang, C., Chao, W.C., and Linardopoulos, S. (2014). APC/C is an essential regulator of centrosome clustering. Nat Commun *5*, 3686.

Du, Y., English, C.A., and Ohi, R. (2010). The kinesin-8 Kif18A dampens microtubule plus-end dynamics. Curr Biol *20*, 374-380.

Elting, M.W., Hueschen, C.L., Udy, D.B., and Dumont, S. (2014). Force on spindle microtubule minus ends moves chromosomes. J Cell Biol *206*, 245-256.

Enos, A.P., and Morris, N.R. (1990). Mutation of a gene that encodes a kinesin-like protein blocks nuclear division in A. nidulans. Cell *60*, 1019-1027.

Euteneuer, U., Jackson, W.T., and McIntosh, J.R. (1982). Polarity of spindle microtubules in Haemanthus endosperm. J Cell Biol *94*, 644-653.

Euteneuer, U., and McIntosh, J.R. (1981). Structural polarity of kinetochore microtubules in PtK1 cells. J Cell Biol *89*, 338-345.

Felgner, H., Frank, R., Biernat, J., Mandelkow, E.M., Mandelkow, E., Ludin, B., Matus, A., and Schliwa, M. (1997). Domains of neuronal microtubule-associated proteins and flexural rigidity of microtubules. J Cell Biol *138*, 1067-1075.

Flindt, R. (2006). Amazing numbers in biology. Springer.

Florian, S., and Mayer, T.U. (2011). Modulated microtubule dynamics enable Hklp2/Kif15 to assemble bipolar spindles. Cell Cycle *10*, 3533-3544.

Fujiwara, T., Bandi, M., Nitta, M., Ivanova, E.V., Bronson, R.T., and Pellman, D. (2005). Cytokinesis failure generating tetraploids promotes tumorigenesis in p53-null cells. Nature *437*, 1043-1047.

Ganem, N.J., and Compton, D.A. (2004). The KinI kinesin Kif2a is required for bipolar spindle assembly through a functional relationship with MCAK. J Cell Biol *166*, 473-478.

Ganem, N.J., Godinho, S.A., and Pellman, D. (2009). A mechanism linking extra centrosomes to chromosomal instability. Nature *460*, 278-282.

Ganem, N.J., Storchova, Z., and Pellman, D. (2007). Tetraploidy, aneuploidy and cancer. Curr Opin Genet Dev *17*, 157-162.

Ganem, N.J., Upton, K., and Compton, D.A. (2005). Efficient mitosis in human cells lacking poleward microtubule flux. Curr Biol *15*, 1827-1832.

Gard, D.L. (1992). Microtubule organization during maturation of Xenopus oocytes: assembly and rotation of the meiotic spindles. Dev Biol *151*, 516-530.

Gard, D.L., and Kirschner, M.W. (1987). A microtubule-associated protein from Xenopus eggs that specifically promotes assembly at the plus-end. J Cell Biol *105*, 2203-2215.

Gascoigne, K.E., and Cheeseman, I.M. (2013). CDK-dependent phosphorylation and nuclear exclusion coordinately control kinetochore assembly state. J Cell Biol *201*, 23-32.

Gascoigne, K.E., and Taylor, S.S. (2008). Cancer cells display profound intra- and interline variation following prolonged exposure to antimitotic drugs. Cancer Cell *14*, 111-122.

Gavet, O., and Pines, J. (2010). Progressive activation of CyclinB1-Cdk1 coordinates entry to mitosis. Dev Cell *18*, 533-543.

Gonczy, P., Pichler, S., Kirkham, M., and Hyman, A.A. (1999). Cytoplasmic dynein is required for distinct aspects of MTOC positioning, including centrosome separation, in the one cell stage Caenorhabditis elegans embryo. J Cell Biol *147*, 135-150.

Good, J.A.S., Berretta, G., Anthony, N.G., and Mackay, S.P. (2015). The discovery and development of Eg5 inhibitors for the clinic. In: Kinesins and Cancer, ed. F. Kozielski: Springer Netherlands, 27-52.

Gorbsky, G.J., and Borisy, G.G. (1989). Microtubules of the kinetochore fiber turn over in metaphase but not in anaphase. J Cell Biol *109*, 653-662.

Goshima, G., Wollman, R., Stuurman, N., Scholey, J.M., and Vale, R.D. (2005). Length control of the metaphase spindle. Curr Biol *15*, 1979-1988.

Grill, S.W., Gonczy, P., Stelzer, E.H., and Hyman, A.A. (2001). Polarity controls forces governing asymmetric spindle positioning in the Caenorhabditis elegans embryo. Nature *409*, 630-633.

Grishchuk, E.L., Molodtsov, M.I., Ataullakhanov, F.I., and McIntosh, J.R. (2005). Force production by disassembling microtubules. Nature *438*, 384-388.

Groen, A. (2013). Microtubule motors: a new hope for kinesin-5 inhibitors? Curr Biol *23*, R617-618.

Hagan, I., and Yanagida, M. (1990). Novel potential mitotic motor protein encoded by the fission yeast cut7+ gene. Nature *347*, 563-566.

Hahn, A.T., Jones, J.T., and Meyer, T. (2009). Quantitative analysis of cell cycle phase durations and PC12 differentiation using fluorescent biosensors. Cell Cycle *8*, 1044-1052.

Heald, R., Tournebize, R., Blank, T., Sandaltzopoulos, R., Becker, P., Hyman, A., and Karsenti, E. (1996). Self-organization of microtubules into bipolar spindles around artificial chromosomes in Xenopus egg extracts. Nature *382*, 420-425.

Heck, M.M., Pereira, A., Pesavento, P., Yannoni, Y., Spradling, A.C., and Goldstein, L.S. (1993). The kinesin-like protein KLP61F is essential for mitosis in Drosophila. J Cell Biol *123*, 665-679.

Hoeijmakers, J.H. (2009). DNA damage, aging, and cancer. N Engl J Med *361*, 1475-1485.

Holland, A.J., and Cleveland, D.W. (2012). Losing balance: the origin and impact of aneuploidy in cancer. EMBO Rep *13*, 501-514.

Houghtaling, B.R., Yang, G., Matov, A., Danuser, G., and Kapoor, T.M. (2009). Op18 reveals the contribution of nonkinetochore microtubules to the dynamic organization of the vertebrate meiotic spindle. Proc Natl Acad Sci U S A *106*, 15338-15343.

Hsu, J.M., Lee, Y.C., Yu, C.T., and Huang, C.Y. (2004). Fbx7 functions in the SCF complex regulating Cdk1-cyclin B-phosphorylated hepatoma up-regulated protein (HURP) proteolysis by a proline-rich region. J Biol Chem *279*, 32592-32602.

Hu, C.K., Coughlin, M., Field, C.M., and Mitchison, T.J. (2008). Cell polarization during monopolar cytokinesis. J Cell Biol *181*, 195-202.

Inoue, S., and Sato, H. (1967). Cell motility by labile association of molecules. The nature of mitotic spindle fibers and their role in chromosome movement. J Gen Physiol *50*, Suppl:259-292.

Kabeche, L., and Compton, D.A. (2013). Cyclin A regulates kinetochore microtubules to promote faithful chromosome segregation. Nature *502*, 110-113.

Kapitein, L.C., Peterman, E.J., Kwok, B.H., Kim, J.H., Kapoor, T.M., and Schmidt, C.F. (2005). The bipolar mitotic kinesin Eg5 moves on both microtubules that it crosslinks. Nature *435*, 114-118.

Kapoor, T.M., Lampson, M.A., Hergert, P., Cameron, L., Cimini, D., Salmon, E.D., McEwen, B.F., and Khodjakov, A. (2006). Chromosomes can congress to the metaphase plate before biorientation. Science *311*, 388-391.

Kapoor, T.M., Mayer, T.U., Coughlin, M.L., and Mitchison, T.J. (2000). Probing spindle assembly mechanisms with monastrol, a small molecule inhibitor of the mitotic kinesin, Eg5. J Cell Biol *150*, 975-988.

Khodjakov, A., Cole, R.W., Oakley, B.R., and Rieder, C.L. (2000). Centrosome-independent mitotic spindle formation in vertebrates. Curr Biol *10*, 59-67.

Khodjakov, A., and Rieder, C.L. (1996). Kinetochores moving away from their associated pole do not exert a significant pushing force on the chromosome. J Cell Biol *135*, 315-327.

Kleyman, M., Kabeche, L., and Compton, D.A. (2014). STAG2 promotes error correction in mitosis by regulating kinetochore-microtubule attachments. J Cell Sci *127*, 4225-4233.

Kollu, S., Bakhoum, S.F., and Compton, D.A. (2009). Interplay of microtubule dynamics and sliding during bipolar spindle formation in mammalian cells. Curr Biol *19*, 2108-2113.

Koshland, D.E., Mitchison, T.J., and Kirschner, M.W. (1988). Polewards chromosome movement driven by microtubule depolymerization in vitro. Nature *331*, 499-504.

Kwon, M., Godinho, S.A., Chandhok, N.S., Ganem, N.J., Azioune, A., Thery, M., and Pellman, D. (2008). Mechanisms to suppress multipolar divisions in cancer cells with extra centrosomes. Genes Dev *22*, 2189-2203.

Lampson, M.A., Renduchitala, K., Khodjakov, A., and Kapoor, T.M. (2004). Correcting improper chromosome-spindle attachments during cell division. Nat Cell Biol *6*, 232-237.

Levesque, A.A., and Compton, D.A. (2001). The chromokinesin Kid is necessary for chromosome arm orientation and oscillation, but not congression, on mitotic spindles. J Cell Biol *154*, 1135-1146.

Li, H.J., Ray, S.K., Singh, N.K., Johnston, B., and Leiter, A.B. (2011). Basic helix-loop-helix transcription factors and enteroendocrine cell differentiation. Diabetes Obes Metab *13 Suppl 1*, 5-12.

Lindqvist, A., Rodriguez-Bravo, V., and Medema, R.H. (2009). The decision to enter mitosis: feedback and redundancy in the mitotic entry network. J Cell Biol *185*, 193-202.

Ly, T., Endo, A., and Lamond, A.I. (2015). Proteomic analysis of the response to cell cycle arrests in human myeloid leukemia cells. Elife *4*.

Maffini, S., Maia, A.R., Manning, A.L., Maliga, Z., Pereira, A.L., Junqueira, M., Shevchenko, A., Hyman, A., Yates, J.R., 3rd, Galjart, N.*, et al.* (2009). Motor-independent targeting of CLASPs to kinetochores by CENP-E promotes microtubule turnover and poleward flux. Curr Biol *19*, 1566-1572.

Magidson, V., O'Connell, C.B., Loncarek, J., Paul, R., Mogilner, A., and Khodjakov, A. (2011). The spatial arrangement of chromosomes during prometaphase facilitates spindle assembly. Cell *146*, 555-567.

Maia, A.R., Garcia, Z., Kabeche, L., Barisic, M., Maffini, S., Macedo-Ribeiro, S., Cheeseman, I.M., Compton, D.A., Kaverina, I., and Maiato, H. (2012). Cdk1 and Plk1 mediate a CLASP2

phospho-switch that stabilizes kinetochore-microtubule attachments. J Cell Biol *199*, 285-301.

Malumbres, M., and Barbacid, M. (2009). Cell cycle, CDKs and cancer: a changing paradigm. Nat Rev Cancer *9*, 153-166.

Manning, A.L., Bakhoum, S.F., Maffini, S., Correia-Melo, C., Maiato, H., and Compton, D.A. (2010). CLASP1, astrin and Kif2b form a molecular switch that regulates kinetochore-microtubule dynamics to promote mitotic progression and fidelity. EMBO J *29*, 3531-3543.

Marcus, A.I., Peters, U., Thomas, S.L., Garrett, S., Zelnak, A., Kapoor, T.M., and Giannakakou, P. (2005). Mitotic kinesin inhibitors induce mitotic arrest and cell death in Taxol-resistant and -sensitive cancer cells. J Biol Chem *280*, 11569-11577.

Mastronarde, D.N., McDonald, K.L., Ding, R., and McIntosh, J.R. (1993). Interpolar spindle microtubules in PTK cells. J Cell Biol *123*, 1475-1489.

McEwen, B.F., Heagle, A.B., Cassels, G.O., Buttle, K.F., and Rieder, C.L. (1997). Kinetochore fiber maturation in PtK1 cells and its implications for the mechanisms of chromosome congression and anaphase onset. J Cell Biol *137*, 1567-1580.

Merdes, A., Ramyar, K., Vechio, J.D., and Cleveland, D.W. (1996). A complex of NuMA and cytoplasmic dynein is essential for mitotic spindle assembly. Cell *87*, 447-458.

Milo, R., Jorgensen, P., Moran, U., Weber, G., and Springer, M. (2010). BioNumbers--the database of key numbers in molecular and cell biology. Nucleic Acids Res *38*, D750-753.

Mitchison, T., and Kirschner, M. (1984). Dynamic instability of microtubule growth. Nature *312*, 237-242.

Mitchison, T.J. (1989). Polewards microtubule flux in the mitotic spindle: evidence from photoactivation of fluorescence. J Cell Biol *109*, 637-652.

Miyamoto, D.T., Perlman, Z.E., Burbank, K.S., Groen, A.C., and Mitchison, T.J. (2004). The kinesin Eg5 drives poleward microtubule flux in Xenopus laevis egg extract spindles. J Cell Biol *167*, 813-818.

Mountain, V., Simerly, C., Howard, L., Ando, A., Schatten, G., and Compton, D.A. (1999). The kinesin-related protein, HSET, opposes the activity of Eg5 and cross-links microtubules in the mammalian mitotic spindle. J Cell Biol *147*, 351-366.

Musacchio, A., and Salmon, E.D. (2007). The spindle-assembly checkpoint in space and time. Nat Rev Mol Cell Biol *8*, 379-393.

Nogales, E., Wolf, S.G., and Downing, K.H. (1998). Structure of the alpha beta tubulin dimer by electron crystallography. Nature *391*, 199-203.

Oki, T., Nishimura, K., Kitaura, J., Togami, K., Maehara, A., Izawa, K., Sakaue-Sawano, A., Niida, A., Miyano, S., Aburatani, H*., et al.* (2014). A novel cell-cycle-indicator, mVenus-p27K-, identifies quiescent cells and visualizes G0-G1 transition. Sci Rep *4*, 4012.

Petry, S., Groen, A.C., Ishihara, K., Mitchison, T.J., and Vale, R.D. (2013). Branching microtubule nucleation in Xenopus egg extracts mediated by augmin and TPX2. Cell *152*, 768-777.

Potapova, T.A., Daum, J.R., Pittman, B.D., Hudson, J.R., Jones, T.N., Satinover, D.L., Stukenberg, P.T., and Gorbsky, G.J. (2006). The reversibility of mitotic exit in vertebrate cells. Nature *440*, 954-958.

Raaijmakers, J.A., Tanenbaum, M.E., and Medema, R.H. (2013). Systematic dissection of dynein regulators in mitosis. J Cell Biol *201*, 201-215.

Raaijmakers, J.A., van Heesbeen, R.G., Meaders, J.L., Geers, E.F., Fernandez-Garcia, B., Medema, R.H., and Tanenbaum, M.E. (2012). Nuclear envelope-associated dynein drives prophase centrosome separation and enables Eg5-independent bipolar spindle formation. EMBO J *31*, 4179-4190.

Reed, S.I. (2003). Ratchets and clocks: the cell cycle, ubiquitylation and protein turnover. Nat Rev Mol Cell Biol *4*, 855-864.

Rieder, C.L. (1981). The structure of the cold-stable kinetochore fiber in metaphase PtK1 cells. Chromosoma *84*, 145-158.

Rieder, C.L., and Cole, R. (2000). Microtubule disassembly delays the G2-M transition in vertebrates. Curr Biol *10*, 1067-1070.

Rogers, G.C., Rogers, S.L., Schwimmer, T.A., Ems-McClung, S.C., Walczak, C.E., Vale, R.D., Scholey, J.M., and Sharp, D.J. (2004). Two mitotic kinesins cooperate to drive sister chromatid separation during anaphase. Nature *427*, 364-370.

Rosner, M., Schipany, K., and Hengstschlager, M. (2013). Merging high-quality biochemical fractionation with a refined flow cytometry approach to monitor nucleocytoplasmic protein expression throughout the unperturbed mammalian cell cycle. Nat Protoc *8*, 602-626.

Santaguida, S., and Amon, A. (2015). Short- and long-term effects of chromosome mis-segregation and aneuploidy. Nat Rev Mol Cell Biol *16*, 473-485.

Santamaria, D., Barriere, C., Cerqueira, A., Hunt, S., Tardy, C., Newton, K., Caceres, J.F., Dubus, P., Malumbres, M., and Barbacid, M. (2007). Cdk1 is sufficient to drive the mammalian cell cycle. Nature *448*, 811-815.

Saunders, A.M., Powers, J., Strome, S., and Saxton, W.M. (2007). Kinesin-5 acts as a brake in anaphase spindle elongation. Curr Biol *17*, R453-454.

Savage, D.C. (1977). Microbial ecology of the gastrointestinal tract. Annu Rev Microbiol *31*, 107-133.

Sawin, K.E., LeGuellec, K., Philippe, M., and Mitchison, T.J. (1992). Mitotic spindle organization by a plus-end-directed microtubule motor. Nature *359*, 540-543.

Segbert, C., Barkus, R., Powers, J., Strome, S., Saxton, W.M., and Bossinger, O. (2003). KLP-18, a Klp2 kinesin, is required for assembly of acentrosomal meiotic spindles in Caenorhabditis elegans. Mol Biol Cell *14*, 4458-4469.

Sharp, D.J., Brown, H.M., Kwon, M., Rogers, G.C., Holland, G., and Scholey, J.M. (2000). Functional coordination of three mitotic motors in Drosophila embryos. Mol Biol Cell *11*, 241-253.

Sherwood, S.W., Rush, D.F., Kung, A.L., and Schimke, R.T. (1994). Cyclin B1 expression in HeLa S3 cells studied by flow cytometry. Exp Cell Res *211*, 275-281.

Sikirzhytski, V., Magidson, V., Steinman, J.B., He, J., Le Berre, M., Tikhonenko, I., Ault, J.G., McEwen, B.F., Chen, J.K., Sui, H.*, et al.* (2014). Direct kinetochore-spindle pole connections are not required for chromosome segregation. J Cell Biol *206*, 231-243.

Sillje, H.H., Nagel, S., Korner, R., and Nigg, E.A. (2006). HURP is a Ran-importin beta-regulated protein that stabilizes kinetochore microtubules in the vicinity of chromosomes. Curr Biol *16*, 731-742.

Stead, E., White, J., Faast, R., Conn, S., Goldstone, S., Rathjen, J., Dhingra, U., Rathjen, P., Walker, D., and Dalton, S. (2002). Pluripotent cell division cycles are driven by ectopic Cdk2, cyclin A/E and E2F activities. Oncogene *21*, 8320-8333.

Stumpff, J., Wagenbach, M., Franck, A., Asbury, C.L., and Wordeman, L. (2012). Kif18A and chromokinesins confine centromere movements via microtubule growth suppression and spatial control of kinetochore tension. Dev Cell *22*, 1017-1029.

Sturgill, E.G., Das, D.K., Takizawa, Y., Shin, Y., Collier, S.E., Ohi, M.D., Hwang, W., Lang, M.J., and Ohi, R. (2014). Kinesin-12 Kif15 targets kinetochore fibers through an intrinsic two-step mechanism. Curr Biol *24*, 2307-2313.

Sturgill, E.G., and Ohi, R. (2013). Kinesin-12 differentially affects spindle assembly depending on its microtubule substrate. Curr Biol *23*, 1280-1290.

Syrovatkina, V., Fu, C., and Tran, P.T. (2013). Antagonistic spindle motors and MAPs regulate metaphase spindle length and chromosome segregation. Curr Biol *23*, 2423-2429.

Tanenbaum, M.E., Macurek, L., Galjart, N., and Medema, R.H. (2008). Dynein, Lis1 and CLIP-170 counteract Eg5-dependent centrosome separation during bipolar spindle assembly. EMBO J *27*, 3235-3245.

Tanenbaum, M.E., Macurek, L., Janssen, A., Geers, E.F., Alvarez-Fernandez, M., and Medema, R.H. (2009). Kif15 cooperates with eg5 to promote bipolar spindle assembly. Curr Biol *19*, 1703-1711.

Tao, W., South, V.J., Zhang, Y., Davide, J.P., Farrell, L., Kohl, N.E., Sepp-Lorenzino, L., and Lobell, R.B. (2005). Induction of apoptosis by an inhibitor of the mitotic kinesin KSP requires both activation of the spindle assembly checkpoint and mitotic slippage. Cancer Cell *8*, 49-59.

Tassan, J.P., Schultz, S.J., Bartek, J., and Nigg, E.A. (1994). Cell cycle analysis of the activity, subcellular localization, and subunit composition of human CAK (CDK-activating kinase). J Cell Biol *127*, 467-478.

Tauchman, E.C., Boehm, F.J., and DeLuca, J.G. (2015). Stable kinetochore-microtubule attachment is sufficient to silence the spindle assembly checkpoint in human cells. Nat Commun *6*, 10036.

Thein, K.H., Kleylein-Sohn, J., Nigg, E.A., and Gruneberg, U. (2007). Astrin is required for the maintenance of sister chromatid cohesion and centrosome integrity. J Cell Biol *178*, 345-354.

Thompson, S.L., and Compton, D.A. (2011). Chromosome missegregation in human cells arises through specific types of kinetochore-microtubule attachment errors. Proc Natl Acad Sci U S A *108*, 17974-17978.

Toso, A., Winter, J.R., Garrod, A.J., Amaro, A.C., Meraldi, P., and McAinsh, A.D. (2009). Kinetochore-generated pushing forces separate centrosomes during bipolar spindle assembly. J Cell Biol *184*, 365-372.

Tran, P.T., Marsh, L., Doye, V., Inoue, S., and Chang, F. (2001). A mechanism for nuclear positioning in fission yeast based on microtubule pushing. J Cell Biol *153*, 397-411.

Uetake, Y., and Sluder, G. (2004). Cell cycle progression after cleavage failure: mammalian somatic cells do not possess a "tetraploidy checkpoint". J Cell Biol *165*, 609-615.

Uetake, Y., and Sluder, G. (2010). Prolonged prometaphase blocks daughter cell proliferation despite normal completion of mitosis. Curr Biol *20*, 1666-1671.

van Heesbeen, R.G., and Medema, R. (2015). Kif15: a useful target for anti-cancer therapy? In: Kinesins and Cancer, ed. F. Kozielski: Springer Netherlands, 77-86.

van Heesbeen, R.G., Tanenbaum, M.E., and Medema, R.H. (2014). Balanced activity of three mitotic motors is required for bipolar spindle assembly and chromosome segregation. Cell Rep *8*, 948-956.

Vanneste, D., Takagi, M., Imamoto, N., and Vernos, I. (2009). The role of Hklp2 in the stabilization and maintenance of spindle bipolarity. Curr Biol *19*, 1712-1717.

Vassilev, L.T. (2006). Cell cycle synchronization at the G2/M phase border by reversible inhibition of CDK1. Cell Cycle *5*, 2555-2556.

Vassilev, L.T., Tovar, C., Chen, S., Knezevic, D., Zhao, X., Sun, H., Heimbrook, D.C., and Chen, L. (2006). Selective small-molecule inhibitor reveals critical mitotic functions of human CDK1. Proc Natl Acad Sci U S A *103*, 10660-10665.

Villerbu, N., Gaben, A.M., Redeuilh, G., and Mester, J. (2002). Cellular effects of purvalanol A: a specific inhibitor of cyclin-dependent kinase activities. Int J Cancer *97*, 761-769.

Vladimirou, E., McHedlishvili, N., Gasic, I., Armond, J.W., Samora, C.P., Meraldi, P., and McAinsh, A.D. (2013). Nonautonomous movement of chromosomes in mitosis. Dev Cell *27*, 60-71.

Walczak, C.E., Gayek, S., and Ohi, R. (2013). Microtubule-depolymerizing kinesins. Annu Rev Cell Dev Biol *29*, 417-441.

Walker, R.A., O'Brien, E.T., Pryer, N.K., Soboeiro, M.F., Voter, W.A., Erickson, H.P., and Salmon, E.D. (1988). Dynamic instability of individual microtubules analyzed by video light microscopy: rate constants and transition frequencies. J Cell Biol *107*, 1437-1448.

Wang, H., Brust-Mascher, I., Civelekoglu-Scholey, G., and Scholey, J.M. (2013). Patronin mediates a switch from kinesin-13-dependent poleward flux to anaphase B spindle elongation. J Cell Biol *203*, 35-46.

Waters, J.C., Mitchison, T.J., Rieder, C.L., and Salmon, E.D. (1996). The kinetochore microtubule minus-end disassembly associated with poleward flux produces a force that can do work. Mol Biol Cell *7*, 1547-1558.

Weinert, T.A., and Hartwell, L.H. (1988). The RAD9 gene controls the cell cycle response to DNA damage in Saccharomyces cerevisiae. Science *241*, 317-322.

Werner, M., Munro, E., and Glotzer, M. (2007). Astral signals spatially bias cortical myosin recruitment to break symmetry and promote cytokinesis. Curr Biol *17*, 1286-1297.

Wieser, S., and Pines, J. (2015). The biochemistry of mitosis. Cold Spring Harb Perspect Biol *7*, a015776.

Winey, M., Mamay, C.L., O'Toole, E.T., Mastronarde, D.N., Giddings, T.H., Jr., McDonald, K.L., and McIntosh, J.R. (1995). Three-dimensional ultrastructural analysis of the Saccharomyces cerevisiae mitotic spindle. J Cell Biol *129*, 1601-1615.

Wittmann, T., Wilm, M., Karsenti, E., and Vernos, I. (2000). TPX2, A novel xenopus MAP involved in spindle pole organization. J Cell Biol *149*, 1405-1418.

Wordeman, L., Wagenbach, M., and von Dassow, G. (2007). MCAK facilitates chromosome movement by promoting kinetochore microtubule turnover. J Cell Biol *179*, 869-879.

Ye, F., Tan, L., Yang, Q., Xia, Y., Deng, L.W., Murata-Hori, M., and Liou, Y.C. (2011). HURP regulates chromosome congression by modulating kinesin Kif18A function. Curr Biol *21*, 1584-1591.

Yi, Q., Zhao, X., Huang, Y., Ma, T., Zhang, Y., Hou, H., Cooke, H.J., Yang, D.Q., Wu, M., and Shi, Q. (2011). p53 dependent centrosome clustering prevents multipolar mitosis in tetraploid cells. PLoS One *6*, e27304.

Yoder, J.H., and Han, M. (2001). Cytoplasmic dynein light intermediate chain is required for discrete aspects of mitosis in Caenorhabditis elegans. Mol Biol Cell *12*, 2921-2933.

Zaytsev, A.V., Sundin, L.J., DeLuca, K.F., Grishchuk, E.L., and DeLuca, J.G. (2014). Accurate phosphoregulation of kinetochore-microtubule affinity requires unconstrained molecular interactions. J Cell Biol *206*, 45-59.

Zhai, Y., Kronebusch, P.J., and Borisy, G.G. (1995). Kinetochore microtubule dynamics and the metaphase-anaphase transition. J Cell Biol *131*, 721-734.

Zhu, C., Lau, E., Schwarzenbacher, R., Bossy-Wetzel, E., and Jiang, W. (2006). Spatiotemporal control of spindle midzone formation by PRC1 in human cells. Proc Natl Acad Sci U S A *103*, 6196-6201.